Published in final edited form as:
Chem Rev. 2009 October ; 109(10): 4760–4779. doi:10.1021/cr900104z.

Structural Biology of Copper Trafficking

Amie K. Boal and **Amy C. Rosenzweig***
Departments of Biochemistry, Molecular Biology and Cell Biology and of Chemistry, Northwestern University, Evanston, IL 60208

1. Introduction

1.1. Background

The use of copper in biological systems coincides with the advent of an oxygen atmosphere about 1.7 billion years ago. The presence of O_2 both allowed the oxidation of insoluble Cu(I) to the more soluble and bioavailable Cu(II) and led to the requirement for a redox active metal with potentials in the 0-800 mV range. Not only did copper meet this need, but the oxidation of Fe(II) to the insoluble Fe(III) form rendered the use of iron more energetically expensive.[1-5] As a result, copper plays a key role in many proteins that react with O_2. Generally, O_2-reactive centers are mononuclear (type 2), dinuclear (type 3), or trinuclear (type 2 and type 3). Well studied mononuclear copper enzymes include the monooxygenases dopamine-β-hydroxylase and peptidylglycine α-hydroxylating monooxygenase as well as oxidases that also contain organic cofactors, such as amine, galactose, and lysyl oxidases.[6] Dinuclear copper proteins include the O_2 carrier hemocyanin and enzymes like tyrosinase and catechol oxidase.[7] Copper also plays a key role in numerous electron transfer proteins. Mononuclear type 1 (blue copper) centers are found in proteins such as plastocyanin and azurin.[8] The multicopper oxidases like laccase, ascorbate oxidase, and ceruloplasmin contain both a catalytic trinuclear type 2/type 3 site and an electron transfer type 1 site.[9,10] The classification of copper centers into types is derived from optical and electron paramagnetic resonance (EPR) spectroscopic properties, and there are some notable exceptions, including the cysteine-bridged dinuclear Cu_A electron transfer site in cytochrome *c* oxidase[11] and nitrous oxide reductase, the tetranuclear catalytic Cu_Z center in nitrous oxide reductase,[12] and the proposed catalytic copper center in particulate methane monooxygenase.[13-15]

The same redox properties that render copper useful in all these metalloproteins can lead to oxidative damage in cells. Reaction of Cu(I) with hydrogen peroxide and re-reduction of Cu (II) by superoxide via Fenton and Haber-Weiss chemistry yields hydroxyl radicals that can damage proteins, lipids, and nucleic acids.[16] Thus, intracellular copper concentrations must be controlled such that copper ions are provided to essential enzymes, but do not accumulate to deleterious levels. In humans, deficiencies in copper metabolism are linked to diseases such as Menkes syndrome, Wilson disease, prion diseases, and Alzheimer's disease.[17] Several classes of proteins, including membrane transporters,[18-20] metallochaperones,[21,22] and metalloregulatory proteins,[23,24] are implicated in copper homeostasis. These proteins have two functions. First, they ensure that copper is provided to the correct proteins and cellular compartments for necessary activities. Second, these proteins detoxify excess copper. Just as copper-containing proteins and enzymes are found in all kingdoms of life, members of these groups of homeostatic proteins are also widespread,[5] and have been structurally and biochemically characterized from eukaryotes and prokaryotes.

*To whom correspondence should be addressed. Phone: 847-467-5301. amyr@northwestern.edu. Fax: 847-467-6489..

1.2. Scope

Understanding how copper is handled in the cell on the molecular level requires knowing the folds of the key proteins and the details of copper coordination, including specific residues involved, location within the protein fold, and metrical parameters. It is only with this information that models for how copper is transferred from one site to another can be formulated. In the last decade, the molecular structures of numerous copper handling proteins or domains thereof have been reported. Cataloging of these structures in the literature has generally been confined to specific organisms, pathways, or techniques.[21,22,25-39] In this review, crystallographic, solution, and cryoelectron microscopic structures of copper chaperones and membrane-bound copper transporters from all kingdoms of life are surveyed in a comprehensive fashion (Tables 1 and 2). Since X-ray absorption spectroscopic (XAS) analyses have contributed significantly to understanding copper coordination by these proteins, these data are included as well. Most of the copper handling proteins described here have been functionally characterized, but function remains putative in some cases. Two important aspects of copper homeostasis, copper metalloregulatory proteins[40] and proteins involved in copper delivery to the mitochondria,[41] are addressed in other contributions to this issue.

2. Overview of Copper Trafficking Pathways

2.1. Eukaryotic Systems

Copper is imported into eukaryotic cells as Cu(I) by members of the Ctr copper transporter family (Figure 1).[42] These membrane transporters, identified in yeast, plants, humans, and other mammals, contain several methionine-rich motifs at their N-termini and conserved cysteine and histidine residues at their C-termini (Figure 2).[18,20,38] Interestingly, Ctr proteins can mediate the uptake of platinum anticancer drugs.[43,44] Once inside the cytosol, soluble Cu(I)-binding proteins called copper chaperones deliver the copper to target proteins via direct protein-protein interactions.[21] It is not clear how the chaperones obtain their Cu(I) cargo, but it may be through a direct interaction with the Ctr transporters.[45]

The copper chaperones for superoxide dismutase (CCS)[36] deliver copper to the antioxidant enzyme Cu,Zn superoxide dismutase (SOD1) (Figure 1).[46] Metallation of SOD1 occurs primarily in the cytosol, but a small amount of SOD1 is localized to the mitochondrial intermembrane space if CCS is also present in the intermembrane space.[47] The Atx1-like chaperones transfer Cu(I) to membrane-bound, metal transporting P_{1B}-type ATPases. The founding member of this chaperone family, yeast Atx1, delivers Cu(I) to Ccc2 in the *trans*-Golgi network.[48] Ccc2 then translocates the copper into secretory vesicles where it is loaded into the enzyme Fet3.[49] The human homolog of Atx1, known as Hah1 or Atox1,[50] delivers copper to the Menkes and Wilson disease ATPases (also known as ATP7A and ATP7B, respectively) (Figure 1) for ultimate incorporation into ceruloplasmin. Fet3 and ceruloplasmin are multicopper oxidases that play a role in iron metabolism by catalyzing the oxidation of Fe(II) to Fe(III) at the plasma membrane.[51] Ccc2 and the Menkes/Wilson disease proteins belong to the P-type ATPase superfamily of integral membrane proteins that couple the energy of ATP hydrolysis to cation translocation across membranes.[52,53] The Cu(I) transporting P_{1B}-type ATPases consist of eight transmembrane (TM) helices, cytoplasmic ATP binding (ATPBD, composed of N and P domains) and actuator domains (A domain), and N-terminal soluble metal binding domains (MBDs) (Figure 3).[54] The number of MBDs varies, ranging from two in Ccc2 to six in the Menkes/Wilson disease proteins.[55,56]

2.2. Prokaryotic Systems

In contrast to eukaryotes, most bacterial copper proteins are housed in the plasma membrane (gram-positive bacteria) or plasma membrane and periplasm (gram-negative bacteria) rather than the cytoplasm.[23,57,58] Specific importers analogous to the eukaryotic Ctr proteins have

not been identified. Bacteria also lack homologs to CCS; SOD1 is found in the periplasm of gram-negative bacteria rather than the cytoplasm. The Cu(I) P_{1B}-type ATPases are widespread in prokaryotes, however. In *E. coli*, the CopA ATPase exports Cu(I) from the cytoplasm to the periplasm (Figure 4).[59] Gram positive bacteria such as *Bacillus subtilis* and *Enterococcus hirae* also utilize Cu(I) transporting ATPases. In *B. subtilis*, CopA effluxes Cu(I) from the cytoplasm[60] whereas in *E. hirae*, CopA is suggested to import Cu(I).[29] All of these CopA proteins contain two MBDs. Both *B. subtilis* and *E. hirae* possess Atx1-like cytoplasmic chaperones, designated CopZ and proposed to deliver Cu(I) to CopA.[29,60] A CopZ homolog has not been identified in *E. coli*. A similar system has been characterized in *Archaeoglobus fulgidus*, a hyperthermophilic archaeon. CopA from *A. fulgidus* exports Cu(I) and contains one N-terminal and one C-terminal MBD, rather than two N-terminal MBDs. The *A. fulgidus* CopZ is also unusual in that it contains an additional 130 amino acids fused to the N-terminus of its 70 residue Atx1-like domain (CopZ-CT).[61]

Two additional copper handling systems have been identified in gram-negative bacteria. The *E. coli* Cus system removes copper from the periplasm (Figure 4).[57] Four proteins are involved: the inner membrane pump CusA, the periplasmic proteins CusB and CusF, and the outer membrane protein CusC.[62] Strains of *E. coli*, *Pseudomonas syringae*, and *Xanthomonas campestris* isolated from copper-rich environments also possess plasmid-encoded systems involved in copper resistance.[57] The *E. coli* plasmid-encoded proteins include the multicopper oxidase PcoA, the outer membrane protein PcoB, the periplasmic proteins PcoC and PcoE, and the inner membrane protein PcoD (Figure 4).[63] The homologous proteins from *P. syringae* are denoted CopABCD.[64] There is no *P. syringae* counterpart to *E. coli* PcoE, and it should be noted that this CopA is a multicopper oxidase, not a Cu(I) transporting ATPase like all other CopA proteins discussed here.

Cyanobacteria represent one exception to the paradigm that copper proteins are not found in the bacterial cytoplasm. These bacteria are photosynthetic and require copper for plastocyanin, which plays a critical role in the photosynthetic electron transport chain.[65] Plastocyanin and cytochrome *c* oxidase are found in thylakoid compartments within the cytoplasm, necessitating a supply of copper to the cytoplasm. In *Synechocystis* PCC 6803, the Cu(I) P_{1B}-ATPase CtaA imports Cu(I). A second ATPase, PacS, imports Cu(I) into the thylakoid, and the Atx1-like copper chaperone ScAtx1 is believed to deliver Cu(I) from CtaA to PacS (Figure 5).[66] CtaA and PacS each have a single MBD.

3. Ctr Transporters

Ctr transporters are the only known system for cellular copper uptake in eukaryotes. Although Ctr proteins have been identified in a wide range of organisms[18] very little information regarding their structure and mechanism is available. The most well studied homologs are the human (hCtr1) and yeast (yCtr1) transporters.[20,42,67] Only hCtr1 has been structurally characterized.[38] hCtr1 is a 23 kDa, 190 amino acid protein that is localized to the plasma and vesicular membranes in most tissue types.[68-70] All Ctr monomers are predicted to contain three transmembrane α-helices, and oligomerization is required for function.[69,71,72] The N-terminus of the protein is extracellular, and the C-terminus resides in the cytoplasm.[70] Methionine-rich motifs have been identified in the N-terminus of hCtr1, as well as in transmembrane helix 2 (TM2) (Figure 2).[20,38] These motifs are implicated in modulating the affinity for copper and rate of transport by hCtr1.[70,73] Conserved cysteine and histidine residues are also present in the C-terminal domain (Figure 2).[73] The mechanism of transport in these proteins is likely passive since their function is unaffected by metabolic inhibitors.[69] The concomitant requirement in yeast for plasma membrane metalloreductases indicates that the substrate for Ctr transporters is likely Cu(I) rather than Cu(II). Finally, Ctr proteins have recently been implicated in cellular uptake of the anticancer drug cisplatin.[43]

3.1. Human Ctr1

A 6 Å resolution projection structure of human Ctr1 (hCtr1) has been determined by cryoelectron microscopy. A variant protein, mutated to eliminate a glycosylation site (Asn15Gln) that is not required for transport function, tagged at the N-terminus with hemagglutinin, and heterologously expressed in *Pichia pastoris* was used.[74] This hCtr1 variant adopts two distinct oligomeric states, of which the larger formed two-dimensional crystals that displayed hexagonal packing, consistent with trimer formation. Cryoelectron microscopy analysis confirmed this quaternary structure assignment and revealed a ~9 Å diameter hole at the three-fold axis, consistent with the proposal that the copper translocation pathway is located at the center of the trimer. In addition, the hCtr1 variant employed in this study crystallized in a double-layered configuration resulting in dimers of trimers. The physiological significance of this phenomenon is unknown. The overall architecture of hCtr1 lies somewhere between that of a traditional monomeric transporter and that of channels,[38] which are generally tetrameric.[75]

The three-dimensional structure of hCtr1 was then determined from the same system to an in plane resolution of 7 Å.[76] From this structure, TM2 was identified as the pore-lining helix, and functionally important methionine residues at its extracellular end were shown to be in close proximity within the trimer. Complementary metal analysis and extended X-ray absorption fine structure (EXAFS) data indicate the presence of two Cu(I) sites, ligated by three sulfur donors. These ligands were proposed to be three symmetry-related methionines and cysteines derived from N-terminal MPM motifs, MX_3M motifs in TM2, and C-terminal HCH motifs. Interestingly, removal of the cysteine residues did not affect the Cu(I) stoichiometry, but resulted in nitrogen coordination, presumably from the flanking histidines. On the basis of these data, a pathway through the pore involving Cu(I) exchange between three-coordinate sites was proposed.

3.2. Yeast Ctr1

The C-terminal soluble domain in yeast Ctr1 (yCtr1) is larger than that found in hCtr1 (125 amino acids versus 11 residues).[67] Whereas the hCtr1 C-terminal domain contains only one cysteine residue that is not essential for copper uptake,[71] the yCtr1 C-terminus contains six cysteines. The shorter mammalian Ctr1 variants can complement yCtr1 knockouts[77] but the presence of a longer cysteine rich C-terminal tail is implicated in modulating the cellular response to excess copper inside the cell.[78] Furthermore, the isolated 126 residue C-terminus is capable of delivering Cu(I) to the Atx1 copper chaperone *in vitro*.[79]

Spectroscopic studies provide some insight into the explicit mode of Cu(I) interaction with the C-terminus of yCtr1.[45] The intensities of optical features associated with Cu-S charge transfer bands increase upon addition of up to four equivalents of Cu(I), and this apparent stoichiometry is altered upon mutagenesis of four of the cysteine residues. EXAFS data are consistent with the presence of three-coordinate Cu(I) with all thiolate ligands. Two major features are observed in the Fourier transforms, one best fit with three Cu-S interactions at 2.25 Å and the second fit with two different Cu-Cu interactions at 2.72 and 2.90 Å. Weaker features at 3.7 Å are also present, and the data are overall consistent with the presence of a tetranuclear Cu $(I)_4(\mu\text{-S-Cys})_6$ cluster. The spectra are very similar to those reported for the regulatory domains of the yeast copper-responsive transcription factors Mac1 and Ace1, both proposed to contain tetranuclear Cu(I) clusters.[80]

4. Atx1-like Chaperones

The Atx1-like family of copper chaperones is highly conserved with members present in a wide variety of organisms ranging from bacteria to higher eukaryotes.[28,56] These proteins are

essential for delivery of Cu(I) to the secretory pathway in eukaryotes[42] and for copper detoxification in prokaryotes.[58] Most Atx1 homologs are ~70 amino acid proteins containing a conserved CXXC motif for metal binding. This motif is also found in the MBDs of Cu(I) transporting P_{1B}-ATPases.[21,56] A wealth of structural information is available for many different members of this family (Table 1), leading to the development of specific models for chaperone-mediated metal transfer.

4.1. Yeast Atx1

The yeast Atx1 homolog has been the subject of detailed structural studies (Table 1). Atx1 from *S. cerevisiae* is a 73 amino acid protein that delivers Cu(I) to the Ccc2 ATPase in the secretory pathway.[48] High resolution X-ray structures have been determined for the Hg(II)-bound and apo forms. Structures of Cu(I)-loaded and apo Atx1 have also been determined by NMR spectroscopy, and the coordination environment of Cu(I)-bound Atx1 has been probed by XAS.

4.1.1. Hg(II)-Atx1 Crystal Structure—The Hg(II)-Atx1 structure was the first X-ray structure of an Atx1-like chaperone. The structure shows that metal-bound Atx1 adopts a βαββαβ overall fold in which the β strands form an antiparallel sheet.[81] The two α helices lie on one side of this sheet. This fold is termed ferredoxin-like[82] and is found in a number of other metalloproteins, including MerP, an Atx1-like protein involved in Hg(II) handling.[83, 84] The CXXC motif is located in the loop connecting β strand 1 and α helix 1. The Hg(II) ion is coordinated by the two cysteine residues (Cys15 and Cys18) at distances of 2.33-2.34 Å. The geometry is nearly linear with a S-Hg-S angle of 167°. The metal binding site is relatively exposed at the protein surface, an important feature for docking with and metal transfer to partner proteins. Also in close proximity to the metal binding site are the side chains of Thr14 and Lys65. Residue Lys65, which is a phenylalanine or proline in the Cu(I) ATPase MBDs, was proposed to modulate metal transfer, and additional surface lysine residues form a positively charged patch for interaction with the partner MBDs from Ccc2. Mutagenesis data support functional roles for these lysine residues.[85]

4.1.2. Apo-Atx1 (Oxidized) Crystal Structure—The structure of the apo form of Atx1 in which the CXXC cysteines form a disulfide bond has been determined to 1.2 Å resolution.[81] The biological relevance of this oxidized form is not clear, but the structure provides information about the flexibility of the metal binding region of Atx1. Comparison of the Hg (II)-bound and apo-Atx1 structures reveals that both proteins adopt the same fold. In the apo structure, the Cys15 Cα atom is displaced 4 Å from its position in the Hg(II)-bound structure to allow for participation in a disulfide bond with Cys18. This shift translates to changes in the position of the metal binding loop between residues 14-18 whereas the remainder of the structure is unaltered. Thus, metal binding likely does not induce large-scale conformational changes.

4.1.3. Cu(I)-Atx1 NMR Structure—The solution structure of Cu(I)-Atx1 exhibits the same overall fold (βαββαβ) as that observed in the crystal structures of Hg(II)-Atx1 and oxidized apo-Atx1.[86] The Cu(I) ion is coordinated by Cys15 and Cys18 with a S-Cu-S angle of 120° ± 40° (Figure 6). This spread in the bond angle could be the result of the diversity of geometries present in the NMR ensemble. In general, it should be noted that solution structures of the Cu (I)-loaded proteins and domains represent models that are consistent with the NMR ensembles; the Cu(I) ions are not detected directly. Solvent accessibility calculations indicate that Cys18 is relatively buried while Cys15 is more solvent exposed. The side chain of Lys65 is close to the sulfur atom of Cys15 whereas in the Hg(II)-Atx1 crystal structure, this side chain is closer to Cys18. The Cu(I) ion in this solution structure is less exposed than the Hg(II) ion in the crystal structure.

4.1.4. Apo-Atx1 (Reduced) NMR Structure—The absence of Cu(I) in the apo reduced solution structure of Atx1 results in an opening of the structure in the vicinity of the metal binding site that is accomplished via subtle translational movements of secondary structure elements.[86] The region surrounding the metal binding site (residues 13-33) displays the largest backbone rmsd values in the ensemble of apo structures, consistent with the idea that this region is conformationally flexible.[81] Very dramatic differences are observed in the coordinating cysteine residues between the Cu(I)- and apo-Atx1 solution structures, although the large backbone deviations in the apo protein ensemble must be considered. In particular, Cys15 flips over to face the exterior of the protein and Cys18 becomes much more solvent accessible, further underscoring the malleability of the metal binding region.

4.1.5. Cu(I)-Atx1 Spectroscopy—The Cu X-ray absorption near edge spectrum (XANES) of copper-loaded Atx1 exhibits a 8984 eV transition feature diagnostic of Cu(I) and no features attributable to Cu(II).[48] The XANES data are most consistent with a trigonal coordination environment. Copper-loaded Atx1 is EPR silent at 77K, confirming the absence of Cu(II). The EXAFS data for Cu(I)-Atx1 were best fit with two sulfur ligands at a Cu-S distance of 2.25 Å and an additional sulfur at 2.40 Å.[48] By contrast, EXAFS and ^{199}Hg NMR studies of Hg(II)-Atx1 indicate the presence of a two-coordinate mercury thiolate complex. These spectroscopic data are consistent with the Atx1 structural data, although the identity of the third ligand detected by EXAFS remains unresolved. Possible candidates for this ligand include an exogenous thiol or a cysteine residue from a second protein molecule.

4.2. Human Atox1

The human Atx1 homologue, Atox1 or Hah1, is a 68 amino acid protein. Its function as a Cu (I) chaperone has been demonstrated by complementation studies in yeast.[87] Atox1 can bind and transfer Cu(I) to the N-terminal MBDs of the Wilson and Menkes ATPases.[88-92] Both X-ray and NMR structures are available for Atox1 (Table 1).

4.2.1. Hg(II)-Atox1 Crystal Structure—Hg(II)-Atox1 crystallizes as a dimer, the two monomers linked by the Hg(II) binding site.[93] The monomers each adopt the canonical βαββαβ structure observed for yeast Atx1 and are nearly identical to each other with a ~0.5 Å rmsd observed for the Cα coordinates. The Hg(II) ion is coordinated by two cysteines from one monomer and one cysteine from the second monomer in a distorted tetrahedral fashion with Hg-S bond lengths of 2.3 Å (Cys12A), 2.5 Å (Cys12B), and 2.5 Å (Cys15A). The sulfur from the fourth cysteine, Cys15B, is 2.8 Å from the Hg(II) ion, a distance too long for a covalent bond. The presence of an extended intermolecular hydrogen bonding network in the vicinity of the metal binding site suggests a mechanism for both stabilization of the three coordinate metal binding site and the protein-protein complex as whole during dimer formation. The capacity for metal-mediated dimerization, in general, suggests a mechanism for partner recognition and metal transfer.

4.2.2. Cd(II)-Atox1 Crystal Structure—The structure of Cd(II)-Atox1 also revealed a metal-bridged dimer.[93] The Cd(II) ion is ligated by four cysteine residues in a tetrahedral geometry with bond distances of 2.4 Å for Cys12A and Cys12B and 2.5 Å for Cys15A and Cys15B. As with the Hg(II)-Atox1 structure, the two monomers are nearly identical in structure.

4.2.3. Cu(I)-Atox1 Crystal Structure—Crystallization of Cu(I)-Atox1 required strict anaerobic conditions, and the structure is the only X-ray structure of an Atx1-like chaperone in the presence of the physiological substrate.[93] Similar to the Hg(II)-Atox1 structure, two Atox1 molecules are coordinated to a single Cu(I) ion via three cysteine residues in a distorted tetrahedral configuration (Figure 7). The Cu-S distances are 2.3 Å for Cys12A, Cys15A, and

Cys12B, and 2.4 Å for Cys15B (could be beyond covalent bonding range). This coordination environment is consistent with the EXAFS data for yeast Atx1.[48] In all three Atox1 structures, an extended hydrogen bonding network in the vicinity of the metal binding site holds the two monomers together. Residue Lys60 (equivalent to Lys65 in yeast Atx1) interacts with the cysteine ligands via a water molecule and might counterbalance the negative charge from the two cysteinates. Collectively, the Atox1 crystal structures suggest that a direct metal transfer mechanism between CXXC motifs on an Atx1-like chaperone and its target MBD[48] is possible (Figure 8). Specifically, the Hg(II)- and Cu(II)-Atox1 structures provide models for transfer intermediates and suggest that the second cysteine in the CXXC motif (Cys15 in Atox1) is important in forming an initial three-coordinate intermediate because it is located on a flexible loop whereas the first cysteine (Cys12 in Atox1) is located on a more rigid α helix.[93]

4.2.4. Apo and Cu(I)-Atox1 NMR Structures—The solution structures of apo and Cu(I)-Atox1 are very similar to the crystal structures.[94] Both monomeric and dimeric forms of Atox1 could be detected in solution. Most of the conformational changes upon Cu(I) binding are localized to the metal binding loop. In contrast to Atx1,[86] only one of the cysteines in the metal binding motif (Cys12) deviates from its Cu(I)-bound position in the apo protein. Residue Lys60 shifts upon Cu(I) binding so that the positively charged side chain is oriented towards the metal binding site, consistent with a role in stabilizing the overall negative charge on the copper ion in two- and three-coordinate Cu(I)-thiolate complexes.[81]

4.2.5. Atox1 Spectroscopy—XAS studies of Atox1 confirm that it binds Cu(I).[95] To determine whether exogenous ligands can coordinate Atox1-bound Cu(I), EXAFS data were collected in the presence and absence of various reductants. For Cu(I)-Atox1 prepared in the absence of reductant, the EXAFS spectrum resembles that of linear, two-coordinate S-Cu-S model complexes and is best fit with two Cu-S distances of 2.16 Å. Addition of exogenous thiols such as glutathione and dithiothreitol (DTT) during copper loading followed by dialysis did not result in the presence of a third ligand. Addition of tris(carboxyethyl)phosphine results in spectra typical of three-coordinate Cu-S/P complexes, however. Exogenous thiols added in vast excess (25x) did result in deviations from two-coordinate geometry. These data support the conclusions drawn from the structural studies: Atx1-like chaperones bind Cu(I) via sulfur ligands in flexible two- or three-coordinate geometries and can likely accommodate additional ligands from small molecules or other proteins.

4.3. Bacterial Atx1 Homologues

The best studied bacterial Atx1 homologues are *B. subtilis* CopZ and *E. hirae* CopZ (Table 1).[29,60] For the *B. subtilis* system, it has been shown that CopZ interacts with CopA *in vivo* and that its deletion results in increased copper sensitivity and decreased copper accumulation.[60] The *E. hirae* CopZ is suggested to interact not only with CopA, but also with the copper-responsive transcription factor CopY.[29]

4.3.1. E. hirae Apo and Cu(I)-CopZ NMR Structures—CopZ from *E. hirae* is a 68 amino acid protein containing the conserved CXXC motif also present eukaryotic Atx1 homologues. The NMR structure of *E. hirae* apo CopZ reveals a well defined (backbone atom rmsd < 0.5 Å) βαββαβ structure.[96] As observed with the eukaryotic apo Atx1-like proteins, the regions of greatest conformational flexibility are localized to the metal binding loop and the N-terminus. Also of note are clusters of positively and negatively charged residues on opposite sides of the protein, suggested to facilitate interactions with different protein partners. Binding of Cu(I) elicits changes in the loop and α helix that house the copper binding site, consistent with what is observed in the eukaryotic Atx1-like chaperone structures. A loss of resonances was observed for Cys11 and Cys14 upon Cu(I) binding so the coordination environment could not be determined from this study. Interestingly, measurement of the T_1/T_2 relaxation times indicates

that *E. hirae* Cu(I)-CopZ displays decreased rotational tumbling when compared to apo CopZ, indicating the presence of oligomers or aggregates upon Cu(I) binding.

4.3.2. B. subtilis Apo and Cu(I)-CopZ NMR Structures—The 73 residue *B. subtilis* CopZ also adopts a βαββαβ fold in the presence and absence of Cu(I).[97,98] Comparison of the apo and Cu(I) structures reveals differences in the vicinity of the Cu(I) binding site. In the reduced apo CopZ structure, few NOEs are observed for the loop and first α helix encompassing the cysteine ligands to Cu(I).[98] A similar phenomenon was observed in the reduced apo yeast Atx1 solution structure and was attributed to increased flexibility or dynamics at that site.[86] Notably, the opposite effect is observed for the *E. hirae* CopZ structures. In the absence of copper, the metal binding region is well defined whereas in the presence of copper, resonances for the key residues are not observed.[96]

In the Cu(I)-CopZ structure, the Cu(I) ion is coordinated by Cys13 and Cys16 with a 115° ± 26° S-Cu-S bond angle.[97] As for the yeast Cu(I)-Atx1 solution structure, this value is indicative of a distorted tetrahedral copper coordination environment possibly achieved via an exogenous third ligand. Also of interest in this variant is the presence of a histidine residue, His15, near the metal binding site. The orientation of the histidine side chain precludes interaction with copper, however. Residues Tyr65 and Met11 undergo dramatic environmental changes when comparing the apo and Cu(I) loaded CopZ structures, becoming more solvent accessible. Tyr65 is the equivalent residue to the lysine adjacent to the Cu(I) site in the eukaryotic Atx homologues (Figure 7). Similar to *E. hirae* CopZ, *B. subtilis* CopZ displays a cluster of positively charged residues on the face of the protein housing the Cu(I) site.

4.3.3. B. subtilis and E. hirae CopZ Spectroscopy—EXAFS data have been reported for *E. hirae* CopZ bound to Cu(I) and Ag(I). The EXAFS for Cu(I)-CopZ are best fit by a three-coordinate all sulfur ligand system with Cu-S distances of 2.24 Å for all three ligands.[99] The identity of the third ligand is unclear because the samples were prepared in sulfur-free buffers. The Ag(I)-CopZ data are best fit with two sulfur ligands with Ag-S distances of 2.39 Å. In the case of *B. subtilis* Cu(I)-CopZ, samples reduced with DTT exhibit spectra typical of three-coordinate sulfur ligation with Cu-S distances of 2.25 Å. The third ligand is assigned to DTT.[100] When Cu(I)-CopZ is reduced by ascorbate, oxygen atoms are evident in the first Cu(I) coordination shell as well as a heavy atom scatterer consistent with formation of an oxygen-bridged dicopper cluster that might be formed upon dimerization of two CopZ molecules. Similar types of spectral features are observed upon addition of acetate or citrate.

4.4. Cyanobacterial Atx1-like Chaperones

The 64 amino acid Atx1 homolog from *Synechocystis* PCC 6803 (ScAtx1) interacts with the PacS and CtaA ATPases, as demonstrated by a bacterial two-hybrid assay, and delivers copper to PacS. Genetic deletion studies indicate that ScAtx1 plays a role in the switch from using iron in cytochrome c_6 to using copper in plastocyanin for photosynthetic electron transport.[101] The structure of ScAtx1 has been investigated via NMR (Table 1) and XAS spectroscopies.

4.4.1. Apo and Cu(I)-ScAtx1 NMR Structures—The solution structures of apo and Cu(I)-ScAtx1 exhibit a βαββα overall fold, similar to that observed for all other Atx1-like structures. ScAtx1 is unique, however, in that it is missing the last β strand.[102,103] Apo-ScAtx1 has a rigid structure with low backbone rmsd values except in the vicinity of the CXXC motif, and appears to be a monomer. The Cu(I) coordination is unusual in Cu(I)-ScAtx1. A histidine residue, His61, coordinates the Cu(I) along with the two cysteines from the CXXC motif. The chemical shift values of the His61 nitrogen atoms are consistent with the presence of a Cu-N bond. Residue His61 corresponds to Tyr65 in the bacterial CopZ homologues and to the

conserved lysine residue in eukaryotic Atx1 chaperones (Figure 7). The conformational state of His61 does not change when comparing the apo and Cu(I)-bound structures.

Relaxation and correlation time measurements indicate that Cu(I)-ScAtx1 forms a symmetric dimer that can be converted to monomers upon addition of DTT.[103] Structural models constrained by bond lengths determined by EXAFS support a histidine- or cysteine-linked structure in which the ligand from one subunit coordinates the Cu(I) ion from the second subunit and vice versa. The two Cu(I) ions in these models maintain a relatively long interatomic distance of 5.5-6 Å. The two models result in identical structures for the monomers, but different orientations of the monomers with respect to each other.

4.4.2. Cu(I)-ScAtx1 Spectroscopy—Cu(I)-ScAtx1 EXAFS data confirm the presence of Cu(I) in the metal binding site.[102] The EXAFS are best fit with a three-coordinate 2S/1N environment with bond lengths of 2.24 Å and 1.93 Å, respectively. Multiple scattering consistent with histidine ligation is observed, and there is no evidence for a short Cu-Cu interaction.

4.5. Archaeal Atx1-like Chaperones

A putative CopZ chaperone was identified in the *Archaeoglobus fulgidus* genome.[61] The 69 amino acid Atx1-like domain in *A. fulgidus* CopZ is preceded by an N-terminal 130 residue domain containing nine conserved cysteine residues and homologous to a class of uncharacterized archaeal proteins. *A. fulgidus* is the only known organism with a sequenced genome in which these two proteins are linked, however. The crystal structure of the N-terminal domain of *A. fulgidus* CopZ (CopZ-NT) (Table 1) reveals the presence of additional metal binding sites.

4.5.1. A. fulgidus CopZ Crystal Structure—The structure of CopZ-NT was determined by X-ray crystallography, and a homology model for the C-terminal Atx1-like domain (CopZ-CT) was generated.[61] The CopZ-CT model has a negatively charged surface patch. CopZ-NT exhibits a novel fold composed of two domains, one containing a mononuclear Zn(II) site and the other containing a [2Fe-2S] cluster. The N-terminal domain of CopZ-NT adopts a βααβββα fold with the Zn(II) ion coordinated tetrahedrally by four cysteine residues derived from the loops connecting the β strands. The Zn(II) ion is likely structural, although it is possible that the physiological metal ion is iron. The C-terminal domain of CopZ-NT is composed entirely of α helices. The [2Fe-2S] cluster found in this domain is coordinated by four cysteine residues located in the loops connecting the helices.

4.5.2. A. fulgidus CopZ Spectroscopy—CopZ-NT exhibits optical spectroscopic features typical of [2Fe-2S] cluster proteins.[61] These features disappear upon reduction with dithionite. EXAFS data confirm the presence of a [2Fe-2S] cluster that is partially reduced in the presence of dithionite. The EPR spectrum of reduced CopZ-NT exhibits two types of signals, of which one is unusual for a $[2Fe\text{-}2S]^{+}$ cluster, and the spin state of the cluster could not be established. The EPR spectra are altered in various cysteine mutants as well as in a sample that was cryoreduced by γ-irradiation. The presence of a redox-active [2Fe-2S] cluster in CopZ-NT could confer upon it the ability to reduce Cu(II). CopZ-NT and CopZ-CT each bind one equivalent of Cu(I), although no copper was detected in the CopZ-NT crystal structure. Reduced CopZ-NT can indeed reduce Cu(II) to Cu(I), and one possibility is that Cu(II) binds near the [2Fe-2S] cluster, is reduced, and then transferred to CopZ-CT for subsequent delivery to CopA and efflux from the cell.[61]

5. Copper Transporting ATPases

Organisms from all kingdoms of life employ P_{1B} -type ATPases to transport copper ions across membranes.[54] In prokaryotes, Cu(I) ATPases are used primarily to export excess copper from the cell, with the exception of cyanobacteria that employ these pumps to shuttle copper into the thylakoids.[66] In eukaryotes, Cu(I) ATPases both efflux excess copper and shuttle copper to the secretory pathway for incorporation into enzymes. Mutations in the human Cu(I) P_{1B}-ATPases, ATP7A and ATP7B, lead to the copper metabolic disorders Menkes syndrome and Wilson disease, respectively.[17] The Cu(I) ATPases consist of eight TM helices, an ATPBD that comprises a nucleotide binding domain (N domain) and a phosphorylation domain (P domain) containing an invariant DKTGT sequence that becomes phosphorylated at the aspartate residue during the ATP hydrolysis cycle.[104] An A-domain, a key link in coupling nucleotide hydrolysis to ion transport, is also present (Figure 3). The most structurally well characterized P-type ATPase is the eukaryotic sarcoplasmic reticulum P_2-type Ca(II) ATPase (SERCA1).[105-107] Crystal structures of SERCA1 have provided much insight into the molecular mechanisms of ion transport. SERCA1 and the Cu(I) specific P_{1B}-ATPases are sufficiently dissimilar that homology modeling is not adequate to understand the mechanism of copper transport by P_{1B}-ATPases. In particular, the P_{1B}-type ATPases contain two fewer TM helices, putative copper coordination sites in the TM region, and soluble MBDs located at the termini.

The Cu(I) binding sites responsible for metal coordination during transport likely involve a cysteine-containing sequence motif (CPC) in TM6 (Figure 3) as well as other key residues in TM7 and TM8. The N-termini comprise one to six MBDs that contain conserved CXXC metal binding sequences.[52,53,56,108] The human Wilson (WLN) and Menkes (MNK) disease proteins contain six N-terminal MBDs, the *Drosophila melanogaster* homolog contains four N-terminal MBDs, the *S. cerevisiae* and *E. coli* homologs each contain two N-terminal MBDs, and the *A. fulgidus* homolog has one N-terminal MBD and one C-terminal MBD. Most bacterial Cu(I) ATPases contain one or two MBDs. The MBDs receive copper ions from metallochaperones,[21,37] participate in ATPase regulation,[109] and facilitate intracellular relocalization.[110] A direct role in Cu(I) delivery to the TM sites has not been established, and in the case of *A. fulgidus* CopA, the CopZ chaperone transfers Cu(I) directly to the TM site.[111] In the absence of copper, the six Wilson protein MBDs interact with the ATPBD.[112] A large amount of genetic, biochemical, and biophysical data suggest that the six MBDs in the human proteins have distinct functions[88,90,110,113-116] that may be related to their copper binding properties and/or ability to interact with Atox1.[92,117] High resolution structural information is not available for any P_{1B}-ATPase in its entirety, although many structures have been determined of isolated soluble domains from various organisms (Table 2).

5.1. Yeast Ccc2 Cu(I) ATPase

The yeast Cu(I) ATPase Ccc2 has two N-terminal soluble MBDs, both of which have been structurally characterized as isolated units in solution. These MBDs have a high degree of sequence similarity to the yeast copper chaperone, Atx1. The two regions of Atx1 homology are separated by a short linker (6 amino acids). The solution structure of the N-terminal MBD (Ccc2a) has been determined and a polypeptide containing both MBDs (Ccc2ab) has been investigated (Table 2).

5.1.1. Apo and Cu(I)-Ccc2a NMR Structures—NMR structures have been determined for Ccc2a in both the Cu(I)-loaded and apo forms.[118] As anticipated from its sequence homology to Atx1-like chaperones, Ccc2a assumes a βαββαβ structure regardless of metal loading. The Cu(I) ion is ligated by the CXXC motif. The S-Cu-S bond angle, without imposing rigid geometric constraints, is calculated to be 119° ± 29°, although a linear geometry could

also be refined. As with the other Atx1-like domain structures, this finding indicates that the Cu(I) binding site may accommodate diverse coordination geometries. Comparison to Atx1 reveals subtle differences in secondary structure that render the Cu(I) site more exposed in Ccc2a. Residue Phe64, which is equivalent to Lys65 in Atx1, may stabilize the metal binding loop. A negatively charged surface patch near the metal binding loop is complementary to the positively charged surface observed on Atx1.[81] The most significant deviations between apo and Cu(I)-Ccc2a occur within the metal binding pocket.[118] One of the Cu(I) ligands, Cys16, retains its conformation in both the apo and Cu(I)-bound forms whereas Cys13 flips away from the interior of the protein and becomes significantly more solvent exposed in the apo structure. Residue Met11, not involved in Cu(I) coordination, also shows significant chemical shift changes upon copper binding, although the orientation of the side chain does not change. This methionine interacts with conserved residues Ile20, Leu37, and Phe64 which together form a hydrophobic pocket surrounding the Cu(I) site.

5.1.2. Ccc2ab NMR Data—An attempt to determine the NMR structure of Ccc2ab, which includes both MBDs, reveals that the overall structure of the first domain (Ccc2a) is not greatly altered by the presence of the second domain (Ccc2b).[119] The second domain itself, however, is not well folded, consistent with the observation that only the first domain in this polypeptide readily binds Cu(I). Refolding of Ccc2ab *in vitro* for these experiments likely explains these results, but it may be that individual MBDs have different dynamic properties or require interaction with other soluble or transmembrane domains to assume the proper fold and function.

5.2. Human Cu(I) ATPases

Humans contain two Cu(I) specific P_{1B}-ATPases, ATP7A or MNK and ATP7B or WLN. Both ATPases contain six N-terminal MBDs. NMR structures have been solved for nearly all the MBDs, either individually or as small multidomain constructs. In addition, the NMR structure of the ATPBD from the Wilson protein has been determined (Table 2).

5.2.1. Apo and Ag(I)-MNK4 NMR Structures—The solution structure of the fourth MBD from the Menkes protein (MNK4) was the first structure of an Atx1-like domain and was determined in the apo and Ag(I)-bound forms.[120] The apo structure exhibits the same ferredoxin-like fold as all the Atx1-like proteins and is well defined except for the metal binding region. The Ag(I)-bound form, used as a Cu(I) mimic to improve stability, is similar to the apo form. The orientation of the cysteine ligands in the CXXC motif is such that the S atoms are 4.8 Å apart and typical of linear, two-coordinate S-Ag-S geometry. The Ag(I) binding site is bordered by the Thr13 and Ser16 side chains, small groups that may help sterically define the metal ion binding pocket. As observed in the Ccc2a structure, conserved hydrophobic residues Ile21, Phe66, and Leu38 engage in packing interactions with residues in the metal-binding loop that may define its structure. Residues Gly11 and Met12, also highly conserved, could further constrain the loop position.

5.2.2. Apo and Cu(I)-MNK2 NMR Structures—The solution structure of the second MBD from the Menkes protein (MNK2) has been reported by two different groups.[121,122] Both structures show that MNK2 resembles other MBDs and Cu(I) chaperones in overall fold and the location of the CXXC site on a solvent exposed loop (Figure 9). Upon copper binding, the most significant chemical shift deviations and conformational changes are localized to the metal-binding loop. Of the two cysteines involved in Cu(I) coordination, the N-terminal Cys20 residue undergoes the most drastic changes in signal intensity, indicating that it likely adopts a much more defined conformation in the metal-bound state. The second ligand, Cys23, remains nearly identical in chemical shift values and signal intensities. The angle calculated

between the Cu(I) atom and cysteine S atoms is 140° ± 40°, indicating some deviation from a two-coordinate linear geometry.

Both MNK2 structures exhibit the hydrophobic packing interactions described for the MNK4 structure.[120-122] The phenylalanine (Figure 9), leucine, and methionine residues that stabilize the metal-binding loop in MNK4 are all conserved in MNK2 and occupy similar positions. Unique to MNK2 is the presence of a GLIG motif at the C-terminal end of the first helix. The glycine residues in this motif are located on the same face of the helix and on the same side of the protein as the copper binding site. This surface feature may be important for protein-protein interactions.

5.2.3. Apo and Cu(I)-MNK1 NMR Structures—The first MBD from MNK (MNK1) is similar to the other structurally characterized MNK MBDs.[123] Structures have been solved in the absence and presence of Cu(I) and differences between the two are limited to the metal binding loop. The calculated S-Cu-S bond angle is 170°, only a slight deviation from linear coordination geometry. The hydrophobic packing interactions with the metal-binding motif are also apparent in this structure. Mutation of the conserved phenylalanine, Phe71, to alanine leads to loss of correlation peaks in the spectra, indicative of partial unfolding.

5.2.4. MNK3 NMR Structure—The third MNK MBD (MNK3) is the most differentiated of the six MNK MBDs in terms of sequence (32% sequence identity with other domains).[124] The NMR data show that this domain also differs the most in structure. In these studies, a variant MNK3 (Lys46Val) was used because it is more stable than wildtype MNK3. MNK3 has the same overall βαββαβ fold as that described for all other MBDs, but the α1 helix is nearly a full turn longer in apo MNK3, the α2 helix is a full turn shorter, and the loop connecting α2 and β4 is much longer on average when compared to other Atx1-like folds. Addition of Cu(I) results in increased conformational flexibility in the metal binding loop as well as loss of secondary structure in α1, β1, and β4. This loss in structural definition upon copper binding is reminiscent of that observed for *E. hirae* CopZ,[96] although MNK3 does not form aggregates.

Substitution of the conserved phenylalanine adjacent to the metal binding loop with a proline residue (Pro66) likely accounts for the observed differences in secondary structure .[124] In this position, the Pro66 acts as a helix cap in α2 while a tyrosine three positions away interacts with the CXXC loop. The overall changes in secondary structure help accommodate this substitution while maintaining the hydrophobic interactions near the metal binding site as observed in all MBD structures.

5.2.5. Apo and Cu(I)-MNK6 and MNK6 Ala629Pro Mutant NMR Structures—A point mutation in the sixth MNK MBD (MNK6), Ala629Pro, has been linked to Menkes disease.[125] This residue is located in the C-terminal β strand of MNK6. NMR structures of both wildtype and Ala629Pro MNK6 have been reported and resemble other MBDs.[126] Pro629 does not disrupt the overall structure and has little effect on the structure of the copper binding site. Instead, the mutant MNK6 appears to undergo minor rearrangements to accommodate the slightly larger proline side chain which, in turn, disrupts the hydrogen bonding network between adjacent strands in the β-sheet structure. The functional consequences of this alteration are slight destabilization of the protein in chemical denaturation experiments and marginal loss in Cu(I) affinity. Although these data do not fully explain the connection between the mutation and human disease, they imply that very subtle structural changes in the MBDs can have dramatic consequences for ATPase function *in vivo*.

5.2.6. MNK456 NMR Data—A construct containing the three C-terminal MNK MBDs (MNK456) was investigated by NMR spectroscopy.[127] The three MBDs are separated by linkers of 30 and 5 amino acids, respectively. *De novo* structure determination could not be

carried out for the entire polypeptide due to signal broadening attributed to excessive conformational exchange, especially in the fifth MBD (MNK5). Comparison of backbone amide chemical shifts to those of the single domains indicates that the folds of the three domains within MNK456 are similar to those of the individual domains. MNK456 exhibits complicated dynamics in solution. MNK4 appears to be much more mobile than domains 5 and 6, probably because the linker between 4 and 5 is much longer than that between 5 and 6. Interestingly, copper loading restrains the reorientation capability of MNK4.

5.2.7. WLN56 NMR Structure—The two C-terminal MBDs from Wilson protein (WLN56) are separated by a very short linker (8 amino acids), similar to MNK56. The solution structure of WLN56 shows that the two domains each exhibit a βαββαβ fold, tumble as a single unit, and are oriented in a fixed fashion with the two CXXC motifs pointing away from each other (Figure 10).[88] The linker is sandwiched between the two domains and does not undergo conformational exchange on the NMR timescale. Apo WLN56 binds Cu(I) with neither alteration of the overall structure of the individual domains nor disruption of the orientation of the domains with respect to each other.

5.2.8. WLN34 NMR Structure—The polypeptide consisting of domains 3 and 4 of WLN (WLN34) and their 31 residue linker has also been characterized by NMR.[128] Each domain is well folded and nearly identical to individual structures of the analogous domains in MNK. The linker region is much more disordered, however. Apo WLN34 displays concentration-dependant aggregation tendencies, as measured via relaxation behavior. Addition of Cu(I) prevents aggregation of domain 4. This phenomenon is consistent with nonspecific interprotein interactions between identical domains that are abolished in domain 4 upon Cu(I) binding, but not in domain 3. As for the other MBDs, Cu(I) loading only perturbs the metal binding region.

5.2.9. WLN ATPBD (N domain) NMR Structure—The N domain of the WLN ATPBD has been structurally characterized by NMR.[129] The isolated N domain is a 17 kDa protein and lacks ATPase activity, although it is capable of binding ATP, ADP, or AMP, which stabilize the protein fragment. The structure was determined in the presence of ATP and reveals a central antiparallel six-stranded β-sheet flanked by two α-helical hairpins (Figure 11). The core structure is compact with the exception of a flexible loop region of ~30 amino acids located at the junction between the β-sheet and one of the α-helical motifs. The sequence corresponding to this unstructured section is unique to mammalian Cu(I) specific P_{1B}-ATPases. The overall fold is quite similar to that of the N domain from the *E. coli* KdpB potassium transporting ATPase.[130]

The N domains of P_{1B}-ATPases have little sequence similarity to the ATP-binding domains in the larger P-type ATPase family, however. In particular, the amino acids that constitute the ATP-binding site in other P-type ATPases are not conserved. Instead, multiple sequence alignment indicates that four invariant residues are present in the Wilson protein N domain: Glu1064, His1069, Gly1099, and Gly1101 (Figure 11). Residue His1069 is mutated to glutamine in ~40% of Wilson disease patients.[131] According to the NMR data, this mutation does not cause major structural changes, but does lead to a reduction in ATP binding affinity. Chemical shift analysis upon ATP binding is consistent with the involvement of these four residues as well as significant overall conformational changes. Very few NOEs were observed between the protein and the ATP molecule. Gly1099 and Gly1101 exhibit especially large chemical shift perturbations when comparing AMP and ATP/ADP binding, indicating that these residues might be close to the ATP phosphate tail.

Docking of ATP based on the NMR distance restraints yielded a model in which the adenine ring largely interacts with His1069, possibly via a hydrogen bonding interaction, as well as with a pair of hydrophobic isoleucine residues (Ile1102 and Ile1180). The sugar group is near

Asn1150 and Gly1149, and the phosphate groups are adjacent to the conserved glycine residues Gly1099 and Gly1101. Conserved residue Glu1064 is located ~5 Å from the imidazole ring of His1069, suggesting a role in positioning the histidine side chain for interaction with the adenine ring. Overall, this arrangement is quite different from that in SERCA1, in which the adenine ring is involved in stacking interactions with aromatic amino acid side chains and the phosphate tail is constrained by interactions with positively charged arginine residues.

5.3. Prokaryotic Cu(I) ATPases

Cu(I) specific P_{1B}-ATPases are widely distributed in prokaryotes.[54] Like eukaryotic systems, structural studies of prokaryotic Cu(I) ATPases are largely limited to soluble domains. Solution structures have been solved for the two N-terminal binding domains of the bacterial *B. subtilis* CopA homologue. X-ray crystal structures have been determined for the N, P, and A domains from the archaeal *A. fulgidus* CopA homologue (Table 2). A low-resolution (17 Å) cryoelectron microscopy structure has also been reported for full-length *A. fulgidus* CopA lacking the C-terminal MBD.

5.3.1. B. subtilis CopA MBD NMR Structures—The MBDs from *B. subtilis* have been investigated by NMR.[132-134] *B. subtilis* CopA has two N-terminal MBDs. Only the second domain is folded within a polypeptide consisting of both domains, and its NMR structure was determined both within this polypeptide and as a separate domain.[132] This second MBD (BsCopAb) exhibits the typical Atx1-like fold, and similar to other MBD structures, differences upon Cu(I) binding are localized to the region containing the CXXC motif. The hydrophobic interactions conserved throughout eukaryotic MBDs are also observed, although the methionine residue proximal to the CXXC motif is relatively disordered in the apo form. A positively charged surface near the metal binding site is complementary to a negatively charged region on the surface of *B. subtilis* CopZ.[97]

The first MBD from *B. subtilis* CopA (BsCopAa) was characterized using a mutant, Ser46Val, which introduces a hydrophobic residue into the core of the protein.[134] Ser46Val BsCopAa has a nearly identical structure to BsCopAb. Interestingly, a Ser46Ala substitution leads to a mixture of folded conformations. The structure of the two domain construct (BsCopAab) with the Ser46Val mutation was also reported.[133] The two domains are connected by a 2 amino acid linker, and thus form a tightly associated, rigid structure in the absence of copper. Relaxation data indicate that the two domain apo protein tumbles in solution as a single unit. The interface between the domains is located on the opposite side of the protein from the copper binding site and is formed via several hydrogen bonding and hydrophobic interactions. The interaction between the two domains has little effect on the overall structure of the individual domains or on the structure of the Cu(I) binding motif though it does affect residues located at the interdomain interface. Some of the residues implicated in hydrogen bonding interactions at the interface are also conserved in domains 5 and 6 of WLN and MNK. Addition of Cu(I) leads to changes similar to those observed upon Cu(I) binding to the individual domains. More recently, the NMR structure of wildtype BsCopAab was determined using a slightly different construct.[135] The structure and orientation of the two domains is similar to that determined for the S46V mutant. In the wildtype BsCopAab, addition of more than one Cu(I) led to dimerization and apparent formation of a Cu(I) cluster.

5.3.2. A. fulgidus CopA ATPBD (N and P Domains) Crystal Structure—The soluble ATPBD from *A. fulgidus* CopA was structurally characterized by X-ray crystallography.[136] Whereas the Wilson ATPBD NMR structure only contained the N domain,[129] both the N and P domains are present in this crystal structure. The two domains form a bean-shaped molecule connected by a hinge region, and the ATP binding site located at the interdomain junction (Figure 12). The orientation of the domains relative to each other resembles that found in the

"closed" state of SERCA1.[137] The hinge region likely dictates the range of conformational states available to the protein, and contains several highly conserved residues, including two residues that are mutated in WLN variants linked to disease.[138]

The N domain, as observed in the Wilson N domain NMR structure,[129] is a six stranded antiparallel β sheet bordered by two α helices on each side (Figure 12).[136] The CopA N domain lacks several loops and structural elements found in the eukaryotic N domains, suggesting that it represents a minimal module for P-type ATP hydrolysis. Although the CopA ATPBD structure was obtained in the absence of nucleotide, the structure closely resembles that of the *E. coli* KdpB N domain bound to AMP-PNP. Superposition of the two structures reveals that five residues, highly conserved throughout P_{1B}-ATPases, likely interact with ATP. Glu457, His462, and Gly492 are predicted to be near the adenine ring, and Gly490 and Gly501 likely interact with the sugar and α-phosphate moieties. The location of these residues is similar to that observed for the analogous residues in the Wilson protein N domain,[129] but different from those observed in other P-type ATPases.

The *A. fulgidus* CopA P domain folds into a six-stranded β sheet flanked by three α helices on each side (Figure 12), the same secondary structure arrangement observed for the SERCA1 P domain.[105] The P domain houses the invariant DKTGT motif, the aspartate residue of which is transiently phosphorylated during the ATP hydrolysis reaction. This phosphorylation site is located near the hinge region at the junction between the N and P domains. The P domain contains a number of residues that are highly conserved among P-type ATPases and many of these are located at the N domain interface. Comparison of this structure with nucleotide-bound SERCA1 structures indicates that many of these conserved residues interact with the phosphate groups or Mg(II) ion required for activity.

5.3.3. A. fulgidus CopA A Domain Crystal Structure—The actuator (A) domain in P-type ATPases is not directly involved in ATP hydrolysis, but undergoes significant conformational changes during the catalytic cycle and is likely involved in coupling the ATP hydrolysis reaction to ion transport across the membrane.[105,139] The A domain from *A. fulgidus* CopA is composed of ten β strands with two α helices at the termini (Figure 13), an overall fold similar to that of the SERCA1 A domain.[140] The terminal helices in the CopA A domain structure are likely cytosolic extensions of the transmembrane helices. A highly conserved GE sequence, which makes contacts to the conserved aspartate in the DKTGT motif in the P domain in the SERCA1 structure, is part of a loop between strands β6 and β7 (Figure 13). A similar interaction is predicted for the CopA A and P domains and seems reasonable on the basis of complementary electrostatic surfaces on the GE loop in the A domain and in the vicinity of the DKTGT motif in the P domain. The SERCA1 A domain also interacts with an N-terminal helix-turn-helix motif.[105] This interaction, which takes place on the opposite side of the protein from the GE loop, may be analogous to a possible interaction between the A domain and the N-terminal MBD in *A. fulgidus* CopA or in P_{1B}-ATPases in general.

5.3.4. A. fulgidus CopA Cryoelectron Microscopy Structure—The structure of full length *A. fulgidus* CopA was determined by cryoelectron microscopy.[141] *A. fulgidus* CopA has two soluble MBDs, one located at the N-terminus and the other located at the C-terminus. To determine the interaction site of the N-terminal MBD with the other soluble domains (A, N, and P), two proteins were analyzed, one lacking the C-terminal MBD (ΔC CopA) and one lacking both MBDs (ΔNΔC CopA). Both CopA variants formed tubular crystals that were analyzed by cryoelectron microscopy at ~17 Å resolution. Comparison of the two structures affords a view of the possible location of the N-terminal MBD. Both structures indicate that CopA forms dimers, the physiological relevance of which is unclear. Assignment of the A, N, and P domains was accomplished by docking the X-ray crystal structures of the individual *A. fulgidus* soluble domains into the cryoelectron microscopy structure and using the full-length

SERCA1 structure as a guide. Comparison of the models for the ΔNΔC CopA and ΔC CopA structures reveals several regions of positive difference density. Some of these are likely due to conformational changes of the A, N, and P domains. One region, located between the N and A domains, appears to be the most likely candidate for the N-terminal MBD. This location is similar to that of the N-terminal helix-turn-helix motif in SERCA1 and is consistent with crosslinking and papain digestion studies of other bacterial CopA homologs.[105,142,143]

6. Complexes Between Atx1-like Chaperones and Target MBDs

A number of solution structural studies have been carried out to monitor copper transfer and complex formation between Atx1-like chaperones and the MBDs from P_{1B}-ATPases. Most of this work has involved mapping interaction surfaces by chemical shift analysis. Representative systems from both eukaryotes and prokaryotes have been investigated.

6.1. *S. cerevisiae* Atx1-Ccc2 MBD NMR Structure

Titrations of Cu(I)-^{15}N Atx1 with apo-Ccc2a and Cu(I)-^{15}N Ccc2a with apo-Atx1 indicate formation of a protein-protein adduct.[144] Based on chemical shift analysis, the structure of Cu(I)-Atx1 in the presence of apo-Ccc2a is intermediate between the apo and Cu(I) forms of Atx1. Major conformational changes are not observed for the two proteins within the adduct. The chemical shift changes were mapped to the protein surfaces, and a model of the complex constructed using these data and the crystal structure of the Cu(I)-Atox1 dimer.[93] This model is consistent with the idea of interactions between complementary electrostatic surfaces.

The NMR structure of a Cu(I)-bridged complex between Atx1 and Ccc2a has also been determined (Figure 14).[145] By systematically mutating the four cysteines in the two proteins, the complex was shown to likely involve tricoordinate Cu(I) coordination by Cys15 from Atx1 and Cys13 and Cys16 from Ccc2a. This finding is consistent with previous models for intermediates based on the Atox1 structures.[93] The structure of the Atx1-Cu(I)-Ccc2a adduct shows that the interface involves hydrophobic interactions near the Cu(I) site and complementary electrostatic interactions between interdigitated charged side chains more distant from the metal site. The two essential cysteine ligands for heterodimer formation, Cys15 from Atx1 and Cys16 from Ccc2a, are the most solvent exposed and remain relatively solvent accessible even within the complex. This structure strongly supports a mechanism of Cu(I) transfer involving ligand exchange reactions (Figure 8).[48,93]

6.2. Human Atox1-WLN or MNK MBD NMR Data

A variety of NMR studies have probed interactions between Atox1 and the WLN and MNK MBDs. MNK2 and MNK5 can accept Cu(I) from Atox1 though complex formation is not detected via NMR.[146] By contrast, surface plasmon resonance data indicate that these MBDs and Atox1 do interact.[113] Failure to detect these complexes on the NMR timescale could be attributed to the lack of electrostatic surface complementarity between Atox1 and these MBDs.

The interaction between multidomain MBD constructs and Atox1 has also been studied by NMR.[88] Titration of Cu(I)-Atox1 with WLN56 results in little copper transfer and no apparent adduct formation, consistent with findings from two-hybrid assays.[90] WLN4 can partially transfer copper to WLN56, however. Transfer at a 1:1 ratio of proteins is ~10% efficient and occurs only to WLN6. At higher ratios, transfer to WLN5 is also observed. No adduct formation between WLN4 and WLN56 is observed. Cu(I)-Atox1 does form complexes with WLN2 and WLN4. The chemical shift changes associated with complex formation are localized to the two α helices and the Cu(I) binding loop. Complex formation with WLN4 was further confirmed in the two domain construct WLN34. Little interaction is observed with WLN3, though both

domains are metallated by Cu(I)-Atox1.[128] Similar studies of MNK456 indicate that domain 4 is the initial site of interaction with Cu(I)-Atox1.[127]

6.3. *B. subtilis* CopZ-CopA MBD NMR Data

Prokaryotic Cu(I) chaperone/MBD complexes have also been detected by NMR. With *B. subtilis* CopZ and BsCopAb, interactions are observed when Cu(I)-CopZ and apo-BsCopAb are mixed in equal proportions.[147] The chemical shift perturbations of apo-BsCopAb upon Cu(I)-CopZ addition resemble Cu(I)-BsCopAb, indicating that CopZ can transfer Cu(I) to BsCopAb and that the Cu(I) ion is largely localized to the BsCopAb binding site rather than the CopZ binding site. The complex formed between the two proteins is in rapid exchange with the monomers in solution. Altered chemical shift values upon complex formation are largely localized to the metal binding site. A model for the complex based on chemical shifts involves complementary electrostatic surfaces and is similar to the Atx1-Ccc2a model,[144] although in this case, the chaperone has a negatively charged surface and the MBD has a positively charged surface.

6.4. *Synechocystis* PCC 6803 Atx1-PacS MBD NMR Data

The interactions between ScAtx1 and the PacS MBD have also been explored by NMR.[148] The apo form of the PacS MBD resembles all the other MBDs in overall structure. Addition of apo PacS MBD to the Cu(I)-ScAtx1 homodimer yields a heterodimer composed of the Cu(I)-PacS MBD and apo ScAtx1. In this complex, the histidine ligand from ScAtx1, His61, is no longer coordinated to copper, and its displacement is proposed to initiate Cu(I) transfer. A model based on chemical shift perturbations suggests that the complex is stabilized by copper bridging and a number of intermolecular hydrogen bonds.

7. PcoC-like Copper Resistance Proteins

Several prokaryotes employ a plasmid encoded copper resistance system to adapt to copper rich environments. In *E. coli*, this resistance mechanism is encoded by the seven gene operon *pcoABCDRSE*.[149] Cells harboring this gene cluster exhibit diminished cellular copper accumulation. PcoA is a multicopper oxidase localized to the periplasm, PcoB and PcoD are outer and inner membrane proteins, respectively, and PcoR and PcoS are regulatory proteins. PcoC and PcoE are soluble periplasmic proteins (Figure 4).[63] PcoC has been structurally characterized (Table 1) and is postulated to interact with PcoA.[150-152] A homologous copper resistance gene cluster, the *copABCDRS* operon, has been identified in several plant pathogens (*P. syringae* and *Xanthomonas campestris*).[64] Cells expressing the *cop* cluster accumulate and sequester copper in the periplasm causing the cells to turn blue in color.[64,153] CopC is the PcoC homologue and has also been structurally characterized (Table 1). PcoC-like proteins differ from the Atx1-like chaperones in their copper binding ligands. Instead of a CXXC motif, PcoC-like proteins contain conserved methionine-rich $[M(X)_nM]_m$ sequences as well as conserved histidine residues. Another important difference is that PcoC-like proteins can bind either Cu(I) or Cu(II).

7.1. *E. coli* PcoC Crystal Structure and Spectroscopy

The crystal structure of apo *E. coli* PcoC was solved in two different space groups, each of which contains two monomers in the asymmetric unit, offering several independent views of the structure.[150] The protein forms a seven-stranded β barrel that is very similar in all monomers. The two monomers in each crystal form are weakly associated and likely result from crystal packing. The two monomers are oriented head-to-head in one crystal form and head-to-tail in the other. The methionine-rich motifs are located on an exposed loop, which sits at the monomer-monomer interface in the head-to-head arrangement, burying seven methionines in close proximity. Clustered at the opposite end of the protein are two conserved

histidine residues as well as the N-terminal amino group of the protein. In the head-to-tail structure, the methionine-rich motifs are solvent exposed.

XAS studies indicate that Cu(I) is coordinated in PcoC by two S and one N/O or two N/O and one S ligand whereas Cu(II) is four-coordinate with three N ligands and one OH_x atom.[151, 154] Given the available copper binding motifs in PcoC, copper likely binds at two distinct sites. The methionine rich loop is the better candidate for the Cu(I) site whereas the conserved histidine residues and N-terminal amino group could satisfy the requirements of the Cu(II) site. The propensity for oligomerization also raises the possibility that ligands could be provided in an intermolecular fashion.

7.2. *P. syringae* CopC NMR Structure and Spectroscopy

P. syringae CopC has been characterized via NMR in the apo, Cu(I), and Cu(II) loaded forms.[155-157] The overall fold is similar to that of PcoC. The potential copper binding motifs are localized at either end of the protein, ~30 Å apart, as they are in PcoC. Addition of Cu(I) results in chemical shift perturbations near the methionine-rich site (B site) whereas addition of Cu (II) results in alterations in the vicinity of the conserved histidine residues (A site). The two sites can be occupied simultaneously. Titration of reducing or oxidizing equivalents into Cu (II) or Cu(I) loaded CopC gives rise to spectral changes consistent with transfer of the newly reduced or oxidized copper ion to its appropriate site.

Assignment of the two sites was facilitated by EXAFS data. The Cu(II)-CopC EXAFS are best fit with two histidines (at equatorial positions and 1.99 Å bond lengths) and two other O/N atoms at 2.83 Å.[155] Relaxation measurements suggest that one of these additional ligands is provided by a water molecule,[157] and the other is likely a side chain oxygen atom from an aspartate or glutamate residue. EXAFS spectra of the Cu(I) loaded protein show that the Cu(I) site is three- or four-coordinate but with two (or three) S ligands and one histidine nitrogen ligand. The environment at the B site could allow Cu(I) binding to one histidine, His48 and two (or three) of four possible methionines. The NMR data did not resolve exactly which side chains are ligands. Furthermore, dynamics measurements indicate that partial aggregation can occur upon Cu(I) binding which would allow for coordination of the metal ion by more than one CopC molecule. Overall, the XAS data for *E. coli* PcoC and *P. syringae* CopC are quite consistent with one another.

7.3. *P. syringae* CopC Crystal Structure

CopC from *P. syringae* was crystallized in the Cu(I)-Cu(II) bound state in two crystal forms at low pH (4.5) and high pH (7.5).[158] All monomers adopt the β-barrel fold observed in the CopC NMR structure. The copper ions occupy sites located within the loops connecting the β strands at either end of the barrel (Figure 15). At low pH, three CopC molecules are present in the asymmetric unit. Each molecule is linked to another monomer in a head-to-head fashion via two Cu(I) centers. Each Cu(I) atom is ligated by four methionine residues at an average distance of 2.3 Å, two contributed from each monomer. Each molecule in the asymmetric unit is additionally linked to its symmetry related partner via the Cu(II) site. The Cu(II) ion is ligated by two histidines (His1 and His91) from one monomer, one histidine from the symmetry related monomer (His48), and a water molecule. The intermolecular interactions result in a copper-linked polymer.

At high pH, a single CopC molecule in the asymmetric unit lies in close proximity to the two-fold crystallographic axis. The Cu(I) site is near the interface between the symmetry related molecules and is ligated by a methionine (Met40) and histidine (His48) residue. A water molecule lies between the two copper sites, but at a distance slightly too long for first sphere coordination. The Cu(II) site is four coordinate with coordination by His1, His91, the amino

terminus, and a water molecule (Figure 15). These data are generally consistent with the XAS results, although the observed copper coordination is affected by formation of molecular interfaces in the crystal. The apo CopC structure was also obtained for the His91Phe CopC variant. Several residues in the Cu(I) binding loop are disordered in this structure though the overall structure is very similar to that observed for the native copper-loaded CopC. Oligomeric interactions are not observed in this structure. Although all the crystallographically characterized molecules have the same fold, differences at the N-terminus and the copper binding loops suggest an inherent flexibility that may facilitate copper transfer to and from partner proteins.

8. E. coli CusF and CusB

The *cusCFBA* operon represents an additional copper resistance system in *E. coli*.[159] The CusA, CusB, and CusC proteins resemble multidrug resistance systems. CusA is an inner membrane pump, CusB is a periplasmic protein, and CusC is an outer membrane protein (Figure 4). These three proteins likely form a complex that pumps copper out of the periplasm driven by a proton gradient. CusF is a small soluble protein proposed to deliver copper to the CusCBA complex or to modulate its transport activity via regulatory interactions.[160] The structure of CusF has been determined by both NMR and crystallography (Table 1). The nature of its metal binding site and its ability to interact with CusB have also been investigated by spectroscopy.

8.1. *E. coli* CusF Structures and Spectroscopy

The 1.5 Å resolution crystal structure of apo CusF reveals a small five stranded β-barrel.[161] The topology is unique among known copper binding proteins and instead resembles the oligonucleotide/oligosaccharide binding (OB) fold. The only three conserved residues among known CusF homologues are His36, Met47, and Met49, all potential copper ligands. These residues are clustered at the top of the β-barrel in strands β2 and β3. NMR spectroscopy was employed to examine structural changes upon addition of metals to apo CusF.[161] Addition of Cu(II) did not result in significant chemical shift changes, but Cu(I) addition affects the entire spectrum, with significant changes occurring at the conserved methionines and histidine. The Cu(I) ion was thus modeled into the histidine/methionine site in a three-coordinate geometry. A tryptophan residue, Trp44, is close to the three ligands. Copper binding was further investigated by EXAFS analysis of Cu(I) loaded CusF.[162] The EXAFS are consistent with three coordinate geometry, but also suggested an additional scatterer, possibly the Trp44 indole ring.

The interaction between Cu(I) and Trp44 was further delineated in high resolution structures of the Ag(I) and Cu(I) loaded forms (Figure 16) of CusF solved in two separate studies.[162, 163] These structures confirm the histidine/methionine cluster as the metal binding site. The metal-bound structures are similar to the apo structure, indicating that Cu(I) and Ag(I) do not perturb the overall fold. The metal binding site is oriented towards the interior of the β-barrel and exhibits trigonal planar geometry. In all structures, Trp44 is located very close to the metal ion (~2.7-2.9 Å for Cu(I), ~2.9-3.3 Å for Ag(I)) (Figure 16). The distances and orientation of the indole ring relative to the metal ion are typical of cation-π interactions. Ultraviolet resonance Raman spectroscopic data are also consistent with a cation-tryptophan π interaction.[163]

8.2. *E. coli* CusB Spectroscopy

The CusB protein binds one Cu(I) or Ag(I) ion. EXAFS data for Cu(I)-CusB are best fit with three Cu-S interactions at 2.29 Å. Since CusB contains no cysteines and nine methionine residues, the ligands are likely methionines, and mutagenesis studies indicate that conserved

residues Met38 and Met36 are required for metal binding whereas loss of Met211, also conserved, leads to a small decrease in metal affinity.[164] Selective selenomethionine labelling experiments in conjunction with EXAFS indicate that CusB and CusF can transfer Cu(I) to each other via specific interactions.[165] Metal transfer occurs in both directions, suggesting similar Cu(I) binding affinities. These properties are reminiscent of Cu(I) transfer between Atx1-like chaperones and Cu(I) P_{1B}-type ATPases and suggest that CusF may deliver periplasmic copper to CusB for efflux through the CusCBA complex.

9. Copper Chaperone for Superoxide Dismutase (CCS)

Copper,zinc superoxide dismutase (SOD1) disproportionates superoxide at a copper/zinc active site and requires the copper chaperone CCS for activation in eukaryotes.[166] SOD1s are homodimers in which each monomer coordinates a copper atom via four histidine ligands. The zinc site is immediately adjacent to the copper center and a histidine residue bridges the two metals.[46] The crystal structure of CCS has been determined for yeast and human homologues and for yeast CCS in complex with yeast superoxide dismutase (Table 1). Copper binding is not observed in the structures, but has been investigated by XAS.

9.1. *S. cerevisiae* CCS Crystal Structure

In yeast, copper transfer occurs via a direct protein-protein interaction between yeast CCS (yCCS) and yeast SOD1 (SOD1) and is required for SOD1 activity *in vivo*.[166,167] The structure of apo yCCS reveals that the 27 kDa protein is divided into three separate domains.[168] The first domain (I) adopts an Atx1-like fold, the second domain (II) is an eight stranded β-barrel with two short α helices, and the third C-terminal domain (III) is disordered in this structure.

Domain I shares 34% sequence homology with Atx1, contains the conserved Cu(I) binding CXXC motif, and adopts the βαββαβ Atx1 fold.[168] The most significant differences between yCCS domain I and Atx1 are found in loop 2 (opposite the copper binding site), which contains one fewer amino acid in yCCS, and loop 5 (proximal to the copper binding loop), which changes conformation in yCCS as it leads into domain II. The residues corresponding to the CXXC motif in yCCS (Cys17 and Cys20) form a disulfide bond in the apo structure. Also in the vicinity of this site is a histidine residue, His16. All of these residues could serve as ligands to copper. As observed in eukaryotic Atx1 chaperones, a conserved lysine (Lys66) is present and oriented towards the copper site. Unlike most Atx1-like proteins, yCCS domain I does not have any positively or negatively charged patches on the face containing the CXXC motif.

The secondary structure elements of domain II resemble those of ySOD1. The most significant differences in structure reside in the loop regions, and indicate that yCCS likely does not contain a metal binding site analogous to the ySOD1 active center. Thus, yCCS domain II cannot catalyze superoxide disproportionation and its structural homology to SOD1 is primarily relevant for partner recognition. Importantly, yCCS is a dimer and its interface, involving largely domain II, is strikingly similar to that present in SOD1 dimers. Four hydrogen bonding interactions are present between the monomers, all of which are conserved in the SOD1 dimer. A large number of hydrophobic interactions are present and many of these are conserved in the SOD1 dimer interface as well. This similarity suggested the possibility of copper delivery by heterodimer formation.[168,169] Domain III, which contains a conserved CXC motif and is important for activity,[170] is disordered in this structure. A structure of domain II alone was also determined and shown to form dimers in solution, leading to the proposal that copper delivery occurs via tetramer formation.[171]

9.2. Human CCS Crystal Structure

Sequence alignment of human CCS (hCCS) and yCCS indicates that hCCS has the same three domain architecture as yCCS. The structure of hCCS domain II has been determined.[172] Four protein molecules are found in the asymmetric unit, though likely only the dimer is physiologically relevant. hCCS domain II has the same general structure as domain II from yCCS as well as that of hSOD, but there are several key differences between the two CCS proteins. Domain II of hCCS retains the loops that define the active site channel and the metal binding sites in human SOD1 (hSOD1). A zinc ion is found at the same site as in hSOD1, but no copper ion is present and one of the four histidine ligands in hSOD1 is not conserved in hCCS. Moreover, a number of other residues required for SOD1 activity are not conserved. One loop, loop 6, is more similar to that in yCCS than that in hSOD1, and houses two arginine residues that created a positively charged surface patch that might facilitate protein-protein interactions.

The dimer interface in hCCS domain II is located on the opposite side of the zinc binding site. As in yCCS, the dimer interaction surface very closely resembles that of the hSOD1 dimer interface (as well as that of yCCS), and is stabilized by four hydrogen bonding interactions and a number of hydrophobic contacts. A pair of positively charged residues, not conserved in hSOD1, are present at the interface in hCCS, similar to that found in yCCS. As postulated for yCCS, the structural properties of hCCS domain II indicate that its primary function is probably SOD1 recognition.

9.3. *S. cerevisiae* yCCS-ySOD1 Heterodimer Crystal Structure

The structure of the yCCS-ySOD1 complex was determined using a catalytically inactive form of ySOD1 in which a histidine copper ligand is substituted with phenylalanine.[173] Each heterodimer contains one ySOD1 molecule and one yCCS molecule (Figure 17).[169,173] The dimer interface is largely confined to domain II in yCCS, though domain III is visible in the structure and makes significant contacts to the loops that constitute the ySOD1 active site channel. Heterodimer formation is accompanied by conformational changes in both ySOD1 and yCCS. Domain I in yCCS is oriented differently relative to domain II when the heterodimer and homodimer structures are compared, indicating that the linker between domain I and II is flexible. Two disulfide bonds are present in domain I in the yCCS homodimer structure,[168] one of which is located in the CXXC copper binding motif, are not observed in the SOD1 heterodimer structure.

Domain II is structurally similar to that found in the yCCS homodimer structure. Domain III consists of a long random coil terminating in a ten residue α helix. Remarkably, domain III contacts the S-S subloop in SOD1 which normally forms a disulfide bond with a β strand cysteine. This disulfide is not present in the heterodimer structure; instead the S-S subloop cysteine forms a disulfide bond with Cys229 in yCCS domain III, resulting in opening of the active site channel in SOD1. A hydrogen bonding interaction between a critical arginine residue in the SOD1 active site channel and a backbone amide in yCCS domain III also results in structural changes near the SOD1 active site. Domain III contains an additional cysteine, and both are required for copper delivery to SOD1.

The yCCS/ySOD heterodimer structure supports the inferences drawn from homodimeric structures of CCS chaperones. Domain I is likely involved in copper uptake and remains distal to the SOD1 interaction interface. Domain II interacts extensively with SOD1 in a fashion similar to that found in the SOD1 and CCS homodimers. Domain III is an extended flexible structure that comes into close contact with the SOD1 copper binding site (Figure 17), indicating that it could serve as a delivery module.

9.4. Spectroscopy of hCCS

hCCS can bind up to 3.5 copper ions per protein molecule.[174] XAS and EPR data indicate that these samples consist of a mixture of Cu(I) and Cu(II) likely bound to heterogeneous sites involving both cysteine and histidine coordination environments. Treatment with reducing agents results in a stoichiometry of two copper ions per hCCS molecule, of which each is in the Cu(I) oxidation state and coordinated by three sulfurs at 2.26 Å and interacting with a second Cu(I) ion at 2.7 Å. The Cu-S distances are typical of three coordinate Cu(I) complexes. Mutagenesis of the cysteine motifs in domains I and III indicates that hCCS probably binds Cu(I) independently at each of these sites.[175,176] The observed cluster is best modeled as a Cu_4S_6 adamantane-like structure.[176] The use of selenocysteine has provided further insight into the nature of this cluster, suggesting that cysteines from both domain II and domain III are involved.[177] The explicit mechanism of copper transfer to the SOD1 active site remains unclear, but could involve the formation of intermolecular copper clusters.[177]

10. Conclusions

In the last decade, significant progress has been made toward understanding copper trafficking at the molecular level. Cryoelectron microscopic and XAS data have provided insight into the trimeric architecture and Cu(I) binding sites of Ctr1. The Atx1-like chaperones and MBDs from Cu(I) ATPases share both an overall βαββαβ fold and a conserved CXXC metal binding motif. The two cysteines coordinate Cu(I) and in some cases, a third ligand is present. The abundance of Atx1-like domain structures combined with the dimeric Atox1 X-ray structure, the Atx1-Ccc2a NMR structure, and extensive chemical shift mapping data, are consistent with an interdomain metal transfer mechanism involving ligand exchange. The structures of the ATP binding and A domains from *A. fulgidus* CopA and of the Wilson N domain have been determined, and together with the various MBD structures, complete the characterization of the Cu(I) ATPase soluble domains. Structures of the bacterial copper resistance proteins PcoC and CopC have provided insight into methionine-rich Cu(I) coordination sites, and reveal an intriguing ability to bind Cu(I) and Cu(II) simultaneously. Finally, the structure of the CusF component of the *E. coli* Cus efflux system reveals a Cu(I) coordination sphere that unexpectedly involves a cation-π interaction with a tryptophan residue.

Despite these advances, a number of questions related to the structure of copper trafficking proteins remain unanswered. These questions pertain to both Cu(I) coordination and protein-protein interactions. For several key players in the pathways, the identities of coordinating ligands, coordination geometries, and metrical parameters remain ambiguous. There are no high resolution crystal structures of Ctr1. For hCtr1, the exact identities and arrangement of the ligands to the two Cu(I) sites[76] are not yet clear. The proposed Cu(I) cluster in the C-terminus of yCtr1[45] has not been characterized crystallographically either. According to EXAFS data, hCCS can form a tetracopper cluster,[176] but a structure of CCS in the presence of Cu(I) has not been determined. One of the most important questions still to be answered regarding Cu(I) coordination is the structure of the TM metal binding sites in the Cu(I) ATPases. While the CPC motif is clearly involved, the stoichiometry of Cu(I) binding, the identities of all the ligands, and their location in the three dimensional structure are not known. A recent mutagenesis and EXAFS study of *A. fulgidus* CopA indicates the presence of two distinct TM Cu(I) binding sites.[178] The first site involves residues Cys280, Cys382, and Tyr683, and the second involves Asn683, Met711, and Ser715, all strictly conserved. Understanding the coordination chemistry of Cu(I) within the membrane is critical to determining the mechanism of transport and the molecular basis of Cu(I) specificity. Moreover, the TM sites may exhibit novel coordination chemistry.

Structural data are also needed to understand the protein-protein interactions involved in copper trafficking pathways. In prokaryotes, details of PcoC and CopC interaction with potential

partner proteins are not clear. While Cu(I) transfer from CusF to CusB has been demonstrated,[165] structural data on the CusF-CusB complex or the whole CusCBA system are not available. In eukaryotes, it is not known how Cu(I) is acquired by Atx1-like and CCS chaperones. There is evidence for Cu(I) transfer from the C-terminus of yCtr1 to yeast Atx1 *in vitro*,[79] but structural details of this docking, if it occurs *in vivo*, are not clear. It may be that CCS can dock with Ctr1 as well. Major issues regarding the Cu(I) ATPases also remain unresolved. Although it has been generally assumed that Cu(I) is transferred from chaperone to MBD to the TM metal binding site of the ATPases, direct transfer from MBD to the TM sites has not been demonstrated. Moreover, recent data for the *A. fulgidus* CopA system demonstrate that Cu(I) is transferred directly from the CopZ chaperone to the CopA TM site.[111] In this scenario, the interactions between Atx1-like chaperones and MBDs may be more important for regulatory interactions. If the Atx1-like chaperones do indeed deliver Cu(I) to the TM site, it is unclear how or where they interact with the ATPases. Finally, little is known about the conformational changes that occur upon ATP hydrolysis and Cu(I) translocation. Although the conformational states may be related to those observed for SERCA1,[139] there are major architectural differences between SERCA1 and the P_{1B}-type ATPases, including different numbers of TM helices and the presence of MBDs. Thus, many challenges remain in the structural biology of copper homeostasis. The last decade of research centered on soluble domains and Cu(I) binding to cysteine and methionine-rich sites. In the next decade, the focus will likely shift to integral membrane transporters and their yet to be discovered Cu(I) coordination chemistry.

Acknowledgments

Research in the authors' laboratory on copper homeostasis is supported by NIH grant GM58518.

Biographies

Amy C. Rosenzweig obtained a B. A. in chemistry from Amherst College in 1988 and a Ph. D. in inorganic chemistry in 1994 from Massachusetts Institute of Technology working with Professor Stephen J. Lippard. After an NIH postdoctoral fellowship at Harvard Medical School, she joined the faculty of Northwestern in 1997 where she is currently a Professor of Biochemistry, Molecular Biology, and Cell Biology and of Chemistry. Research interests include structural and biophysical studies of copper trafficking proteins and characterization of integral membrane proteins that oxidize methane to methanol.

Amie K. Boal is a Portland, Oregon native who received her B. A. in chemistry from Pomona College in 2002. In 2008, she received a Ph. D. in chemistry at the California Institute of Technology in the laboratory of Professor Jacqueline K. Barton. Currently, Amie is a postdoctoral scholar in Professor Amy Rosenzweig's laboratory at Northwestern where she is examining interactions between platinum-based anticancer therapeutics and human copper homeostasis proteins.

Abbreviations

A domain, actuator domain of P_{1B}-type ATPase
ATP7A, Menkes syndrome Cu(I) P_{1B}-type ATPase
ATP7B, Wilson disease Cu(I) P_{1B}-type ATPase
ATPBD, ATP binding domain of P_{1B}-type ATPase
BsCopAa, first N-terminal MBD of *B. subtilis* CopA
BsCopAab, both N-terminal MBDs of *B. subtilis* CopA
BsCopAb, second N-terminal MBD of *B. subtilis* CopA
Ccc2a, first N-terminal MBD of yeast Ccc2 Cu(I) P_{1B}-type ATPase
Ccc2ab, both N terminal-MBDs of yeast Ccc2 Cu(I) P_{1B}-type ATPase
CCS, copper chaperone for superoxide dismutase
CopZ-CT, C-terminal domain of *A. fulgidus* CopZ chaperone
CopZ-NT, N-terminal Atx1-like domain of *A. fulgidus* CopZ chaperone
DTT, dithiothreitol
EPR, electron paramagnetic resonance spectroscopy
EXAFS, extended X-ray absorption fine structure
hCCS, human copper chaperone for superoxide dismutase
hCtr1, human Ctr1 transporter
hSOD1, human copper,zinc superoxide dismutase
MBD, metal binding domain of P_{1B}-type ATPase
MNK, Menkes syndrome protein or ATP7A
MNK1, first N-terminal MBD of MNK
MNK2, second N-terminal MBD of MNK
MNK3, third N-terminal MBD of MNK
MNK4, fourth N-terminal MBD of MNK
MNK456, fourth, fifth, and sixth N-terminal MBDs of MNK
MNK5, fifth N-terminal MBD of MNK
MNK6, sixth N-terminal MBD of MNK
N domain, nucleotide binding domain of ATPBD of P_{1B}-type ATPase
P domain, phosphorylation domain of ATPBD of P_{1B}-type ATPase
SERCA1, sarcoplasmic reticulum P_2-type Ca(II) ATPase
SOD1, copper,zinc superoxide dismutase
TM, transmembrane
WLN, Wilson disease protein or ATP7B
WLN56, fifth and sixth N-terminal MBDs of WLN
WLN34, third and fourth N-terminal MBDs of WLN
XANES, X-ray absorption near edge structure
XAS, X-ray absorption spectroscopy
yCCS, yeast copper chaperone for superoxide dismutase
yCtr1, yeast Ctr1 transporter
ySOD1, yeast copper,zinc superoxide dismutase

References

(1). Crichton RR, Pierre J-L. Biometals 2001;14:99. [PubMed: 11508852]
(2). da Silva, J. J. R. Fraústo; Williams, RJP. The biological chemistry of the elements. Vol. Second ed. Oxford University Press; Oxford: 2001.
(3). Kaim W, Rall J. Angew. Chem. Int. Ed. Engl 1996;35:43.
(4). Ochiai EI. J. Chem. Ed 1986;63:942.
(5). Ridge PG, Zhang Y, Gladyshev VN. PLoS ONE 2008;3:e1378. [PubMed: 18167539]
(6). MacPherson IS, Murphy MEP. Cell. Mol. Life Sci 2007;64:2887. [PubMed: 17876515]
(7). Gerdemann C, Eicken C, Krebs B. Acc. Chem. Res 2002;35:183. [PubMed: 11900522]

(8). Dennison C. Coord. Chem. Rev 2005;249:3025.
(9). Nakamura K, Go N. Cell. Mol. Life Sci 2005;62:2050. [PubMed: 16091847]
(10). Quintanar L, Stoj C, Taylor AB, Hart PJ, Kosman DJ, Solomon EI. Acc. Chem. Res 2007;40:445. [PubMed: 17425282]
(11). Beinert H. Eur. J. Biochem 1997;245:521. [PubMed: 9182986]
(12). Chen P, Gorelsky SI, Ghosh S, Solomon EI. Angew. Chem. Int. Ed 2004;43:4132.
(13). Balasubramanian R, Rosenzweig AC. Acc. Chem. Res 2007;40:573. [PubMed: 17444606]
(14). Chan SI, Yu SSF. Acc. Chem. Res 2008;41:969. [PubMed: 18605740]
(15). Hakemian AS, Rosenzweig AC. Ann. Rev. Biochem 2007;76:223. [PubMed: 17328677]
(16). Halliwell B, Gutteridge JMC. Biochem. J 1984;219:1. [PubMed: 6326753]
(17). Mercer JFB. Trends Molec. Med 2001;7:64. [PubMed: 11286757]
(18). Puig S, Thiele DJ. Curr. Op. Chem. Biol 2002;6:171.
(19). Lutsenko S, Petris MJ. J. Membr. Biol 2003;191:1. [PubMed: 12532272]
(20). Maryon EB, Molloy SA, Zimnicka AM, Kaplan JH. Biometals 2007;20:355. [PubMed: 17211679]
(21). Rosenzweig AC. Acc. Chem. Res 2001;34:119. [PubMed: 11263870]
(22). Rosenzweig AC. Chem. Biol 2002;9:673. [PubMed: 12079778]
(23). Tottey S, Harvie DR, Robinson NJ. Acc. Chem. Res 2005;38:775. [PubMed: 16231873]
(24). Winge DR. Adv. Prot. Chem 2002;60:51.
(25). Rosenzweig AC, O'Halloran TV. Curr. Op. Chem. Biol 2000;4:140.
(26). Huffman DL, O'Halloran TV. Annu. Rev. Biochem 2001;70:677. [PubMed: 11395420]
(27). Opella SJ, DeSilva TM, Veglia G. Curr. Op. Chem. Biol 2002;6:217.
(28). Elam JS, Thomas ST, Holloway SP, Taylor AB, Hart PJ. Adv. Prot. Chem 2002;60:151.
(29). Solioz M, Stoyanov JV. FEMS Microbiol. Rev 2003;27:183. [PubMed: 12829267]
(30). Banci L, Rosato A. Acc. Chem. Res 2003;36:215. [PubMed: 12641479]
(31). Markossian KA, Kurganov BI. Biochemistry-Moscow 2003;68:827. [PubMed: 12948382]
(32). Finney LA, O'Halloran TV. Science 2003;300:931. [PubMed: 12738850]
(33). Cavet JS, Borrelly GPM, Robinson NJ. FEMS Microbiol. Rev 2003;27:165. [PubMed: 12829266]
(34). Arnesano F, Banci L, Bertini I, Ciofi-Baffoni S. Eur. J. Inorg. Biochem 2004:1583.
(35). Arnesano F, Banci L, Bertini I, Martinelli M. J. Proteome Res 2005;4:63. [PubMed: 15707358]
(36). Culotta VC, Yang M, O'Halloran TV. Biochim. Biophys. Acta 2006;1763:747. [PubMed: 16828895]
(37). Singleton C, LeBrun NE. Biometals 2007;20:275. [PubMed: 17225061]
(38). De Feo CJ, Aller SG, Unger VM. Biometals 2007;20:705. [PubMed: 17211682]
(39). Lutsenko S, Gupta A, Burkhead JL, Zuzel V. Arch. Biochem. Biophys 2008;476:22. [PubMed: 18534184]
(40). Giedroc DP. Chem. Rev. 2009in press
(41). Winge DR. Chem. Rev. 2009in press
(42). Kim B-E, Nevitt T, Thiele DJ. Nature Chem. Biol 2008;4:176. [PubMed: 18277979]
(43). Ishida S, Lee J, Thiele DJ, Herskowitz I. Proc. Natl. Acad. Sci USA 2002;99:14298. [PubMed: 12370430]
(44). Safaei R, Howell SB. Critical Rev. Onc. Hem 2005;53:13.
(45). Xiao Z, Loughlin F, George GN, Howlett GJ, Wedd AG. J. Am. Chem. Soc 2004;126:3081. [PubMed: 15012137]
(46). Bertini I, Mangani S, Viezzoli MS. Adv. Inorg. Chem 1997;45:127.
(47). Field LS, Furukawa Y, O'Halloran TV, Culotta VC. J. Biol. Chem 2003;278:28052. [PubMed: 12748182]
(48). Pufahl RA, Singer CP, Peariso KL, Lin S-J, Schmidt P, Culotta VC, Penner-Hahn JE, O'Halloran TV. Science 1997;278:853. [PubMed: 9346482]
(49). Yuan DS, Stearman R, Dancis A, Dunn T, Beeler T, Klausner RD. Proc. Natl. Acad. Sci. USA 1995;92:2632. [PubMed: 7708696]

(50). Hung IH, Casareno RLB, Labesse G, Matthews FS, Gitlin JD. J. Biol. Chem 1998;273:1749. [PubMed: 9430722]
(51). Hellman NE, Gitlin JD. Ann. Rev. Nutr 2002;22:439. [PubMed: 12055353]
(52). Lutsenko S, Kaplan JH. Biochemistry 1995;34:15607. [PubMed: 7495787]
(53). Axelsen KB, Palmgren MG. J. Mol. Evol 1998;46:84. [PubMed: 9419228]
(54). Argüello JM, Eren E, González-Guerrero M. Biometals 2007;20:233. [PubMed: 17219055]
(55). Solioz M, Vulpe C. Trends Biochem. Sci 1996;21:237. [PubMed: 8755241]
(56). Arnesano F, Banci L, Bertini I, Ciofi-Baffoni S, Molteni E, Huffman DL, O'Halloran TV. Genome Res 2002;12:255. [PubMed: 11827945]
(57). Rensing C, Grass G. FEMS Microbiol. Rev 2003;27:197. [PubMed: 12829268]
(58). Osman D, Cavet JS. Adv. Appl. Microbiol 2008;65:217. [PubMed: 19026867]
(59). Rensing C, Fan B, Sharma R, Mitra B, Rosen BP. Proc. Natl. Acad. Sci. USA 2000;97:652. [PubMed: 10639134]
(60). Radford DS, Kihlken MA, Borrelly GP, Harwood CR, Le Brun NE, Cavet JS. FEMS Microbiol. Lett 2003;220:105. [PubMed: 12644235]
(61). Sazinsky MH, LeMoine B, Orofino M, Davydov R, Bencze KZ, Stemmler TL, Hoffman BM, Argüello JM, Rosenzweig AC. J. Biol. Chem 2007;282:25950. [PubMed: 17609202]
(62). Grass G, Rensing C. J. Bacteriol 2001;183:2145. [PubMed: 11222619]
(63). Brown NL, Barrett SR, Camakaris J, Lee BTO, Rouch DA. Mol. Microbiol 1995;17:1153. [PubMed: 8594334]
(64). Cha J-S, Cooksey DA. Proc. Natl. Acad. Sci., USA 1991;88:8915. [PubMed: 1924351]
(65). Merchant SS, Allen MD, Kropat J, Moseley JL, Long JC, Tottey S, Terauchi AM. Biochim. Biophys. Acta 2006;1763:578. [PubMed: 16766055]
(66). Tottey S, Rich PR, Rondet SA, Robinson NJ. J. Biol. Chem 2001;276:19999. [PubMed: 11264284]
(67). Dancis A, Haile D, Yuan DS, Klausner RD. J. Biol. Chem 1994;269:25660. [PubMed: 7929270]
(68). Zhou B, Gitschier J. Proc. Natl. Acad. Sci. USA 1997;94:7481. [PubMed: 9207117]
(69). Lee J, Peña MMO, Nose Y, Thiele DJ. J. Biol. Chem 2002;277:4380. [PubMed: 11734551]
(70). Klomp AE, Juijn JA, van der Gun LT, van den Berg IE, Berger R, Klomp LW. Biochem. J 2003;370:881. [PubMed: 12466020]
(71). Eisses JF, Kaplan JH. J. Biol. Chem 2002;277:29162. [PubMed: 12034741]
(72). Aller SG, Eng ET, De Feo CJ, Unger VM. J. Biol. Chem 2004;279:53435. [PubMed: 15385536]
(73). Eisses JF, Kaplan JH. J. Biol. Chem 2005;280:37159. [PubMed: 16135512]
(74). Aller SG, Unger VM. Proc. Natl. Acad. Sci USA 2006;103:3627. [PubMed: 16501047]
(75). Gouaux E, Mackinnon R. Science 2005;310:1461. [PubMed: 16322449]
(76). De Feo CJ, Aller SG, Siluvai GS, Blackburn NJ, Unger VM. Proc. Natl. Acad. Sci. USA 2009;106:4237. [PubMed: 19240214]
(77). Lee J, Prohaska JR, Dagenais SL, Glover TW, Thiele DJ. Gene 2000;254:87. [PubMed: 10974539]
(78). Wu X, Sinani D, Kim H, Lee J. J. Biol. Chem 2009;284:4112. [PubMed: 19088072]
(79). Xiao Z, Wedd AG. Chem. Commun 2002:588.
(80). Brown KR, Keller GL, Pickering IJ, Harris HH, George GN, Winge DR. Biochemistry 2002;41:6469. [PubMed: 12009910]
(81). Rosenzweig AC, Huffman DL, Hou MY, Wernimont AK, Pufahl RA, O'Halloran TV. Structure 1999;7:605. [PubMed: 10404590]
(82). Hubbard TJP, Murzin AG, Brenner SE, Chothia C. Nucleic Acids Res 1997;25:236. [PubMed: 9016544]
(83). Serre L, Rossy E, Pebay-Peyroula E, Cohen-Addad C, Coves J. J. Mol. Biol 2004;339:161. [PubMed: 15123428]
(84). Steele RA, Opella SJ. Biochemistry 1997;36:6885. [PubMed: 9188683]
(85). Portnoy ME, Rosenzweig AC, Rae T, Huffman DL, O'Halloran TV, Culotta VC. J. Biol. Chem 1999;274:15041. [PubMed: 10329707]

(86). Arnesano F, Banci L, Bertini I, Huffman DL, O'Halloran TV. Biochemistry 2001;40:1528. [PubMed: 11327811]

(87). Klomp LWJ, Lin S-J, Yuan DS, Klausner RD, Culotta VC, Gitlin JD. J. Biol. Chem 1997;272:9221. [PubMed: 9083055]

(88). Achila D, Banci L, Bertini I, Bunce J, Ciofi-Baffoni S, Huffman DL. Proc. Natl. Acad. Sci. USA 2006;103:5729. [PubMed: 16571664]

(89). Hamza I, Schaefer M, Klomp LWJ, Gitlin JD. Proc. Natl. Acad. Sci. USA 1999;96:13363. [PubMed: 10557326]

(90). Larin D, Mekios C, Das K, Ross B, Yang A-S, Gilliam TC. J. Biol. Chem 1999;274:28497. [PubMed: 10497213]

(91). Walker JM, Tsivkovskii R, Lutsenko S. J. Biol. Chem 2002;277:27953. [PubMed: 12029094]

(92). Yatsunyk LA, Rosenzweig AC. J. Biol. Chem 2007;282:8622. [PubMed: 17229731]

(93). Wernimont AK, Huffman DL, Lamb AL, O'Halloran TV, Rosenzweig AC. Nature Struct. Biol 2000;7:766. [PubMed: 10966647]

(94). Anastassopoulou I, Banci L, Bertini I, Cantini F, Katsari E, Rosato A. Biochemistry 2004;43:13046. [PubMed: 15476398]

(95). Ralle M, Lutsenko S, Blackburn NJ. J. Biol. Chem 2003;278:23163. [PubMed: 12686548]

(96). Wimmer R, Herrmann T, Solioz M, Wüthrich K. J. Biol. Chem 1999;274:22597. [PubMed: 10428839]

(97). Banci L, Bertini I, Conte RD, Markey J, Ruiz-Dueñas FJ. Biochemistry 2001;40:15660. [PubMed: 11747441]

(98). Banci L, Bertini I, Del Conte R. Biochemistry 2003;42:13422. [PubMed: 14621987]

(99). Cobine PA, George GN, Jones CE, Wickramasinghe WA, Solioz M, Dameron CT. Biochemistry 2002;41:5822. [PubMed: 11980486]

(100). Banci L, Bertini I, Del Conte R, Mangani S, Meyer-Klaucke W. Biochemistry 2003;42:2467. [PubMed: 12600214]

(101). Tottey S, Rondet SAM, Borrelly GPM, Robinson PJ, Rich PR, Robinson NJ. J. Biol. Chem 2002;277:5490. [PubMed: 11739376]

(102). Borrelly GP, Blindauer CA, Schmid R, Butler CS, Cooper CE, Harvey I, Sadler PJ, Robinson NJ. Biochem. J 2004;378:293. [PubMed: 14711369]

(103). Banci L, Bertini I, Ciofi-Baffoni S, Su XC, Borrelly GP, Robinson NJ. J. Biol. Chem 2004;279:27502. [PubMed: 15075318]

(104). Moller JV, Nissen P, Sorensen TL, le Maire M. Curr. Opin. Struct. Biol 2005;15:387. [PubMed: 16009548]

(105). Toyoshima C, Nakasako M, Nomura H, Ogawa H. Nature 2000;405:647. [PubMed: 10864315]

(106). Toyoshima C, Nomura H. Nature 2002;418:605. [PubMed: 12167852]

(107). Toyoshima C, Nomura H, Tsuda T. Nature 2004;432:361. [PubMed: 15448704]

(108). Rensing C, Ghosh M, Rosen BP. J. Bacteriol 1999;181:5891. [PubMed: 10498699]

(109). Mandal AK, Argüello JM. Biochemistry 2003;42:11040. [PubMed: 12974640]

(110). Strausak D, LaFontaine S, Hill J, Firth SD, Lockhart PJ, Mercer JFB. J. Biol. Chem 1999;274:11170. [PubMed: 10196202]

(111). González-Guerrero M, Argüello JM. Proc. Natl. Acad. Sci. USA 2008;105:5992. [PubMed: 18417453]

(112). Tsivkovskii R, MacArthur BC, Lutsenko S. J. Biol. Chem 2001;276:2234. [PubMed: 11053407]

(113). Strausak D, Howie MK, Firth SD, Schlicksupp A, Pipkorn R, Multhaup G, Mercer JFB. J. Biol. Chem 2003;278:20821. [PubMed: 12679332]

(114). Huster D, Lutsenko S. J. Biol. Chem 2003;278:32212. [PubMed: 12794172]

(115). Voskoboinik I, Strausak D, Greenough M, Brooks H, Petris M, Smith S, Mercer JF, Camakaris J. J. Biol. Chem 1999;274:22008. [PubMed: 10419525]

(116). Forbes JR, Hsi G, Cox DW. J. Biol. Chem 1999;274:12408. [PubMed: 10212214]

(117). Wernimont AK, Yatsunyk LA, Rosenzweig AC. J. Biol. Chem 2004;279:12269. [PubMed: 14709553]

(118). Banci L, Bertini I, Ciofi-Baffoni S, Huffman DL, O'Halloran TV. J. Biol. Chem 2001;276:8415. [PubMed: 11083871]

(119). Banci L, Bertini I, Chasapis CT, Rosato A, Tenori L. Biochem. Biophys. Res. Commun 2007;364:645. [PubMed: 17961510]

(120). Gitschier J, Moffat B, Reilly D, Wood WI, Fairbrother WJ. Nature Struct. Biol 1998;5:47. [PubMed: 9437429]

(121). Jones CE, Daly NL, Cobine PA, Craik DJ, Dameron CT. J. Struct. Biol 2003;143:209. [PubMed: 14572476]

(122). Banci L, Bertini I, Del Conte R, D'Onofrio M, Rosato A. Biochemistry 2004;43:3396. [PubMed: 15035611]

(123). DeSilva TM, Veglia G, Opella SJ. Proteins 2005;61:1038. [PubMed: 16211579]

(124). Banci L, Bertini I, Cantini F, DellaMalva N, Herrmann T, Rosato A, Wuthrich K. J. Biol. Chem 2006;281:29141. [PubMed: 16873374]

(125). Tumer Z, Lund C, Tolshave J, Vural B, Tonnesen T, Horn N. Am. J. Hum. Genet 1997;60:63. [PubMed: 8981948]

(126). Banci L, Bertini I, Cantini F, Migliardi M, Rosato A, Wang S. J .Mol. Biol 2005;352:409. [PubMed: 16083905]

(127). Banci L, Bertini I, Cantini F, Chasapis CT, Hadjiliadis N, Rosato A. J. Biol. Chem 2005;280:38259. [PubMed: 16172131]

(128). Banci L, Bertini I, Cantini F, Rosenzweig AC, Yatsunyk LA. Biochemistry 2008;47:7423. [PubMed: 18558714]

(129). Dmitriev O, Tsivkovskii R, Abildgaard F, Morgan CT, Markley JL, Lutsenko S. Proc. Natl. Acad. Sci. USA 2006;103:5302. [PubMed: 16567646]

(130). Haupt M, Bramkamp M, Coles M, Altendorf K, Kessler H. J. Mol. Biol 2004;342:1547. [PubMed: 15364580]

(131). Ferenci P. Aliment. Pharmacol. Ther 2004;19:157. [PubMed: 14723607]

(132). Banci L, Bertini I, Ciofi-Baffoni S, D'Onofrio M, Gonnelli L, Marhuenda-Egea FC, Ruiz-Duenas FJ. J. Mol. Biol 2002;317:415. [PubMed: 11922674]

(133). Banci L, Bertini I, Ciofi-Baffoni S, Gonnelli L, Su XC. J. Biol. Chem 2003;278:50506. [PubMed: 14514665]

(134). Banci L, Bertini I, Ciofi-Baffoni S, Gonnelli L, Su XC. J. Mol. Biol 2003;331:473. [PubMed: 12888353]

(135). Singleton C, Banci L, Ciofi-Baffoni S, Tenori L, Kihlken MA, Boetzel R, Le Brun NE. Biochem. J 2008;411:571. [PubMed: 18215122]

(136). Sazinsky MH, Mandal AK, Argüello JM, Rosenzweig AC. J. Biol. Chem 2006;281:11161. [PubMed: 16495228]

(137). Toyoshima C, Mizutani T. Nature 2004;430:529. [PubMed: 15229613]

(138). Cox DW, Moore SD. J. Bioenerg. Biomembr 2002;34:333. [PubMed: 12539960]

(139). Toyoshima C, Inesi G. Ann. Rev. Biochem 2004;73:269. [PubMed: 15189143]

(140). Sazinsky MH, Agarwal S, Argüello JM, Rosenzweig AC. Biochemistry 2006;45:9949. [PubMed: 16906753]

(141). Wu CC, Rice WJ, Stokes DL. Structure 2008;16:976. [PubMed: 18547529]

(142). Lubben M, Portmann R, Kock G, Stoll R, Young MM, Solioz M. Biometals 2009;22:363. [PubMed: 18979168]

(143). Hatori Y, Majima E, Tsuda T, Toyoshima C. J. Biol. Chem 2007;282:25213. [PubMed: 17616523]

(144). Arnesano F, Banci L, Bertini I, Cantini F, Ciofi-Baffoni S, Huffman DL, O'Halloran TV. J. Biol. Chem 2001;276:41365. [PubMed: 11500502]

(145). Banci L, Bertini I, Cantini F, Felli IC, Gonnelli L, Hadjiliadis N, Pierattelli R, Rosato A, Voulgaris P. Nature Chem. Biol 2006;2:367. [PubMed: 16732294]

(146). Banci L, Bertini I, Ciofi-Baffoni S, Chasapis CT, Hadjiliadis N, Rosato A. FEBS J 2005;272:865. [PubMed: 15670166]

(147). Banci L, Bertini I, Ciofi-Baffoni S, Del Conte R, Gonnelli L. Biochemistry 2003;42:1939. [PubMed: 12590580]

(148). Banci L, Bertini I, Ciofi-Baffoni S, Kandias NG, Robinson NJ, Spyroulis GA, Su X-C, Tottey S, Vanarotti M. Proc. Natl. Acad. Sci. USA 2005;103:8320. [PubMed: 16707580]

(149). Tetaz TJ, Luke RKJ. J. Bacteriol 1983;154:1263. [PubMed: 6343346]

(150). Wernimont AK, Huffman DL, Finney LA, Demeler B, O'Halloran TV, Rosenzweig AC. J. Biol. Inorg. Chem 2003;8:185. [PubMed: 12459914]

(151). Huffman DL, Huyett J, Outten FW, Doan PE, Hoffman BM, O'Halloran TV. Biochemistry 2002;41:10046. [PubMed: 12146969]

(152). Djoko KY, Xiao Z, Wedd AG. Chembiochem 2008;9:1579. [PubMed: 18536063]

(153). Cooksey DA. FEMS Microbiol. Rev 1994;14:381. [PubMed: 7917425]

(154). Huffman DL, Pearlso KL, Penner-Hahn JE, O'Halloran TV. J. Am. Chem. Soc 2003;125:342. [PubMed: 12517140]

(155). Arnesano F, Banci L, Bertini I, Mangani S, Thompsett AR. Proc. Natl. Acad. Sci. U S A 2003;100:3814. [PubMed: 12651950]

(156). Arnesano F, Banci L, Bertini I, Thompsett AR. Structure 2002;10:1337. [PubMed: 12377120]

(157). Arnesano F, Banci L, Bertini I, Felli IC, Luchinat C, Thompsett AR. J. Am. Chem. Soc 2003;125:7200. [PubMed: 12797793]

(158). Zhang L, Koay M, Mahert MJ, Xiao Z, Wedd AG. J. Am. Chem. Soc 2006;128:5834. [PubMed: 16637653]

(159). Munson GP, Lam DL, Outten FW, O'Halloran TV. J. Bacteriol 2000;182:5864. [PubMed: 11004187]

(160). Franke S, Grass G, Rensing C, Nies DH. J .Bacteriol 2003;185:3804. [PubMed: 12813074]

(161). Loftin IR, Franke S, Roberts SA, Weichsel A, Heroux A, Montfort WR, Rensing C, McEvoy MM. Biochemistry 2005;44:10533. [PubMed: 16060662]

(162). Loftin IR, Franke S, Blackburn NJ, McEvoy MM. Protein Sci 2007;16:2287. [PubMed: 17893365]

(163). Xue Y, Davis AV, Balakrishnan G, Stasser JP, Staehlin BM, Focia P, Spiro TG, Penner-Hahn JE, O'Halloran TV. Nature Chem. Biol 2008;4:107. [PubMed: 18157124]

(164). Bagai I, Liu W, Rensing C, Blackburn NJ, McEvoy MM. J. Biol. Chem 2007;282:35695. [PubMed: 17893146]

(165). Bagai I, Rensing C, Blackburn NJ, McEvoy MM. Biochemistry 2008;47:11408. [PubMed: 18847219]

(166). Rae TD, Schmidt PJ, Pufahl RA, Culotta VC, O'Halloran TV. Science 1999;284:805. [PubMed: 10221913]

(167). Culotta VC, Klomp LWJ, Strain J, Casareno RLB, Krems B, Gitlin JD. J. Biol. Chem 1997;272:23469. [PubMed: 9295278]

(168). Lamb AL, Wernimont AK, Pufahl RA, O'Halloran TV, Rosenzweig AC. Nature Struct. Biol 1999;6:724. [PubMed: 10426947]

(169). Lamb AL, Torres AS, O'Halloran TV, Rosenzweig AC. Biochemistry 2000;39:14720. [PubMed: 11101286]

(170). Schmidt PJ, Rae TD, Pufahl RA, Hamma T, Strain J, O'Halloran TV, Culotta VC. J. Biol. Chem 1999;274:23719. [PubMed: 10446130]

(171). Hall LT, Sanchez RJ, Holloway SP, Zhu H, Stine JE, Lyons TJ, Demeler B, Schirf V, Hansen JC, Nersissian AM, Valentine JS, Hart PJ. Biochemistry 2000;39:3611. [PubMed: 10736160]

(172). Lamb AL, Wernimont AK, Pufahl RA, O'Halloran TV, Rosenzweig AC. Biochemistry 2000;39:1589. [PubMed: 10677207]

(173). Lamb AL, Torres AS, O'Halloran TV, Rosenzweig AC. Nature Struct. Biol 2001;8:751. [PubMed: 11524675]

(174). Eisses JF, Stasser JP, Ralle M, Kaplan JH, Blackburn NJ. Biochem 2000;39:7337. [PubMed: 10858280]

(175). Stasser JP, Eisses JF, Barry AN, Kaplan JH, Blackburn NJ. Biochemistry 2005;44:3143. [PubMed: 15736924]

(176). Stasser JP, Siluvai GS, Barry AN, Blackburn NJ. Biochemistry 2007;46:11845. [PubMed: 17902702]

(177). Barry AN, Clark KM, Otoikhian A, van der Donk WA, Blackburn NJ. Biochemistry 2008;47:13074. [PubMed: 19007184]

(178). González-Guerrero M, Eren E, Rawat S, Stemmler TL, Argüello JM. J. Biol. Chem 2008;283:29753. [PubMed: 18772137]

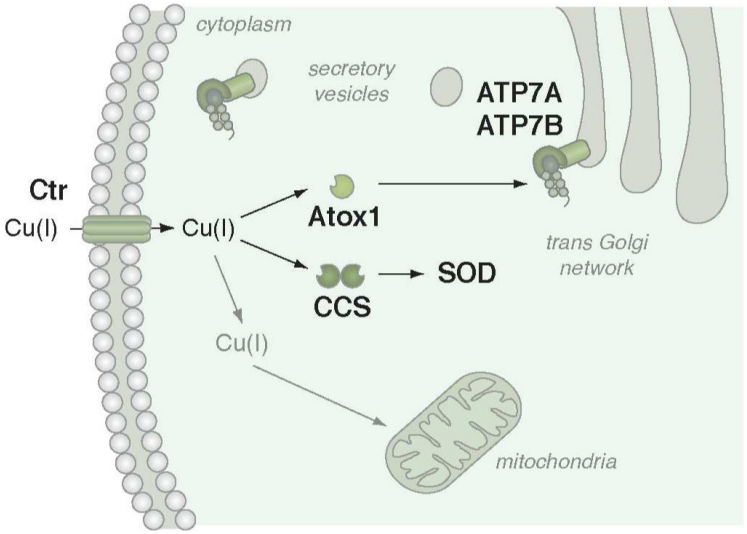

Figure 1.
Copper trafficking pathways in humans.

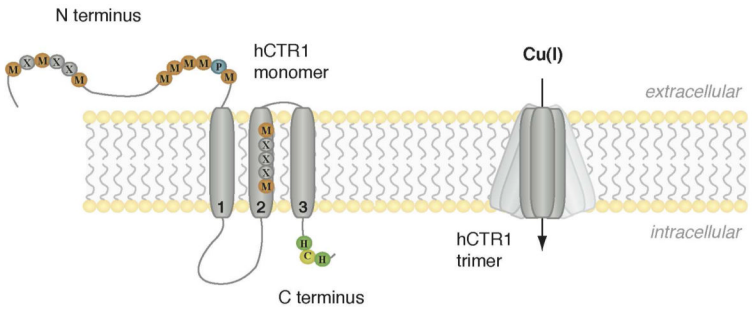

Figure 2.
Overall architecture of hCtr1.

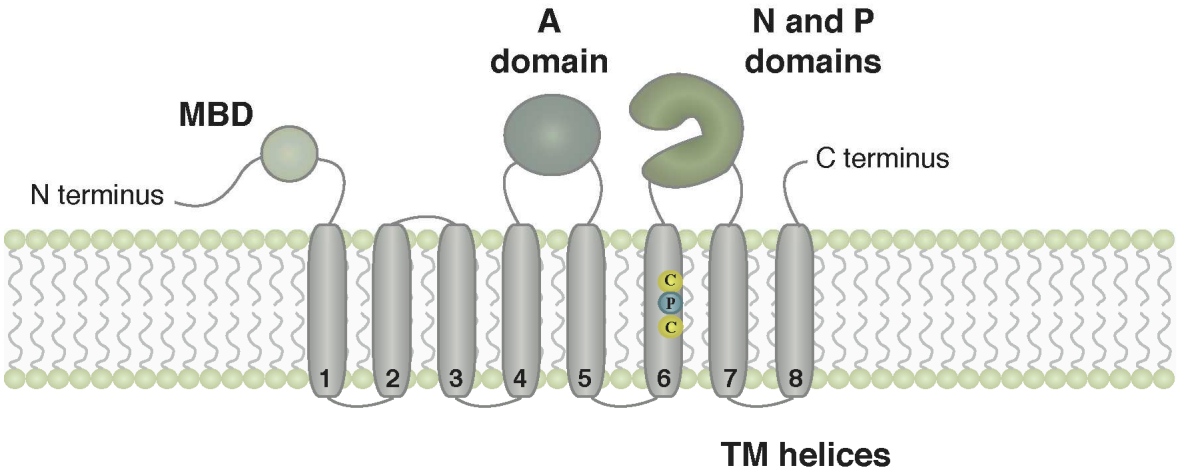

Figure 3.
Overall architecture of Cu(I) P_{1B}-type ATPases. The number of MBDs at the N-terminus ranges from one to six, depending on the organism.

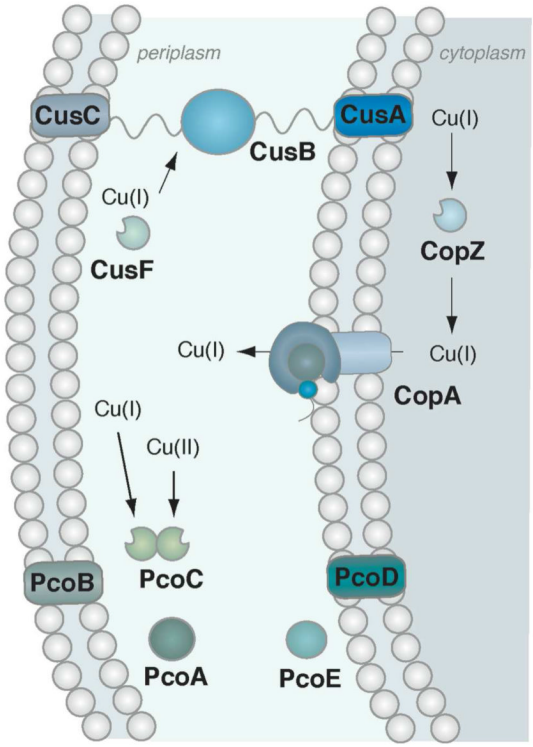

Figure 4.
Copper trafficking pathways in bacteria. CopA ATPases are found in both gram-positive and gram-negative (shown here) bacteria. A CopZ homolog is not found in *E. coli*, but is found in the gram-positive bacteria *B. subtilis* and *E. hirae*. The Pco (also known as Cop) and Cus systems are specific to gram-negative bacteria.

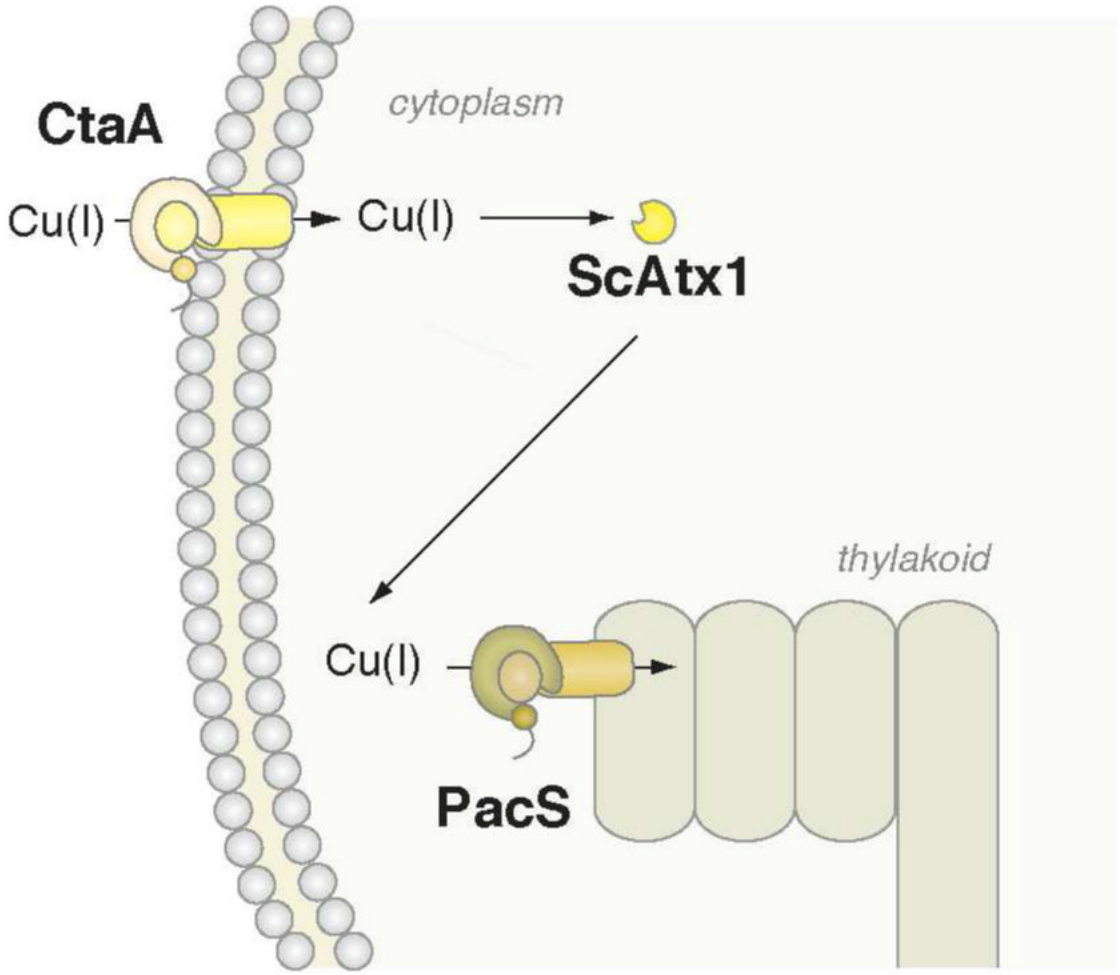

Figure 5.
Copper trafficking pathways in the cyanobacterium *Synechocystis* PCC 6803.

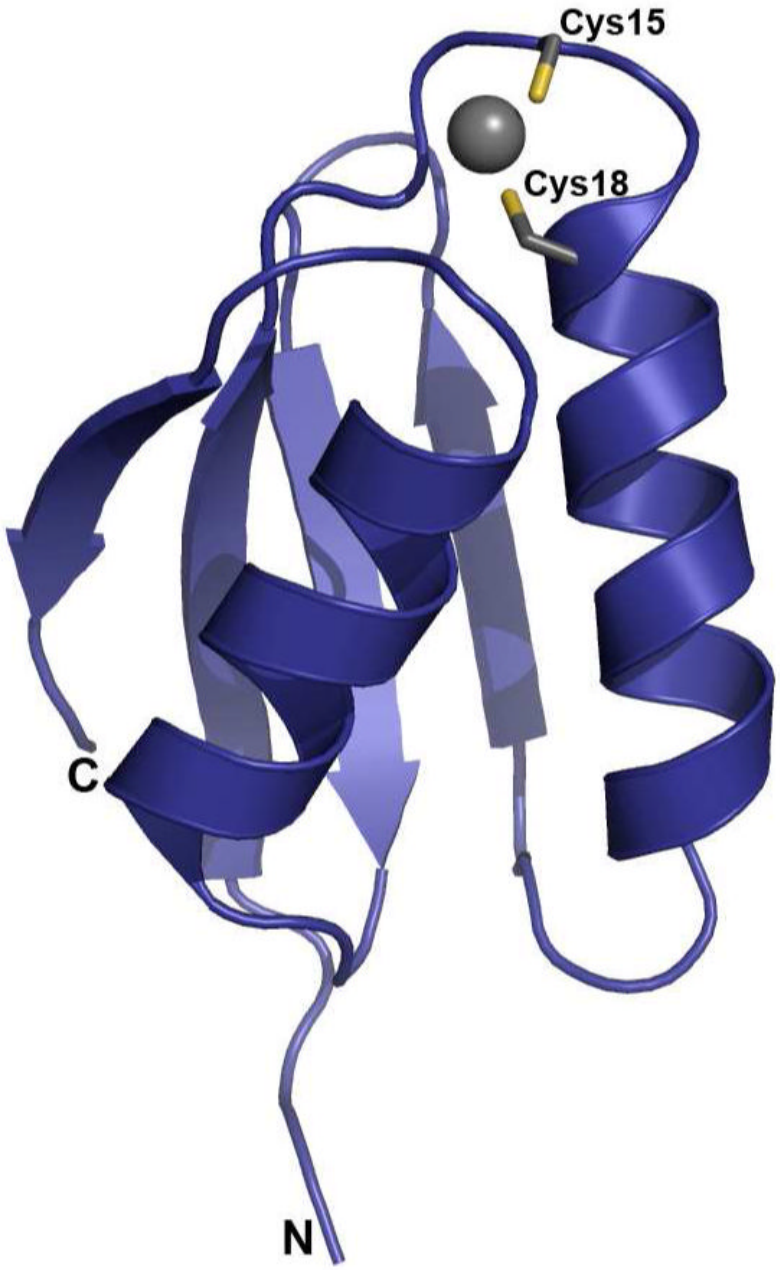

Figure 6.
Solution structure of Cu(I)-Atx1 (PDB accession code 1FD8). The Cu(I) ion is shown as a gray sphere and the two coordinating cysteine residues are shown as sticks.

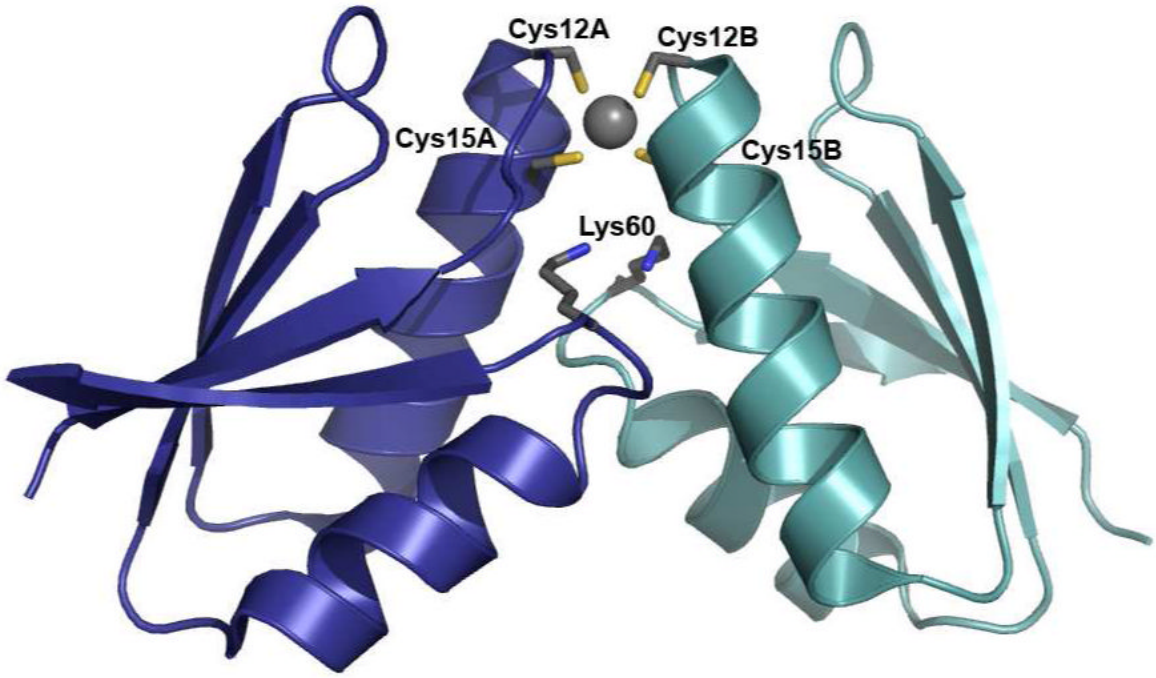

Figure 7.
Crystal structure of Cu(I)-Atox1 (PDB accession code 1FEE). The two monomers are shown in dark blue and cyan and the Cu(I) ion is shown as a gray sphere. Coordinating cysteine residues and adjacent lysine residues are shown as sticks.

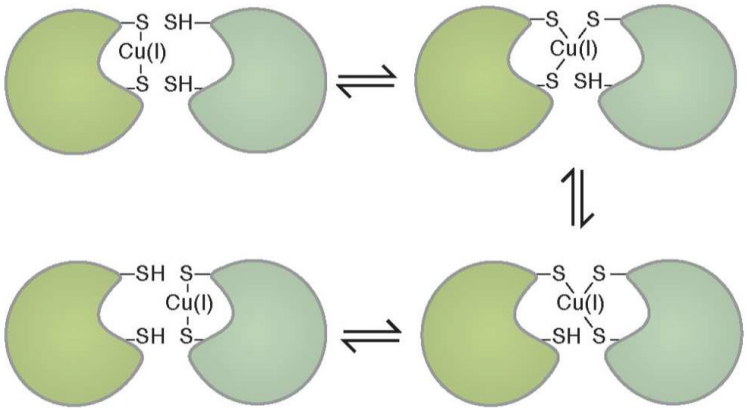

Figure 8.
Proposed mechanism of Cu(I) transfer between an Atx1-like chaperone and a N-terminal MBD of a Cu(I) P_{1B}-type ATPase.

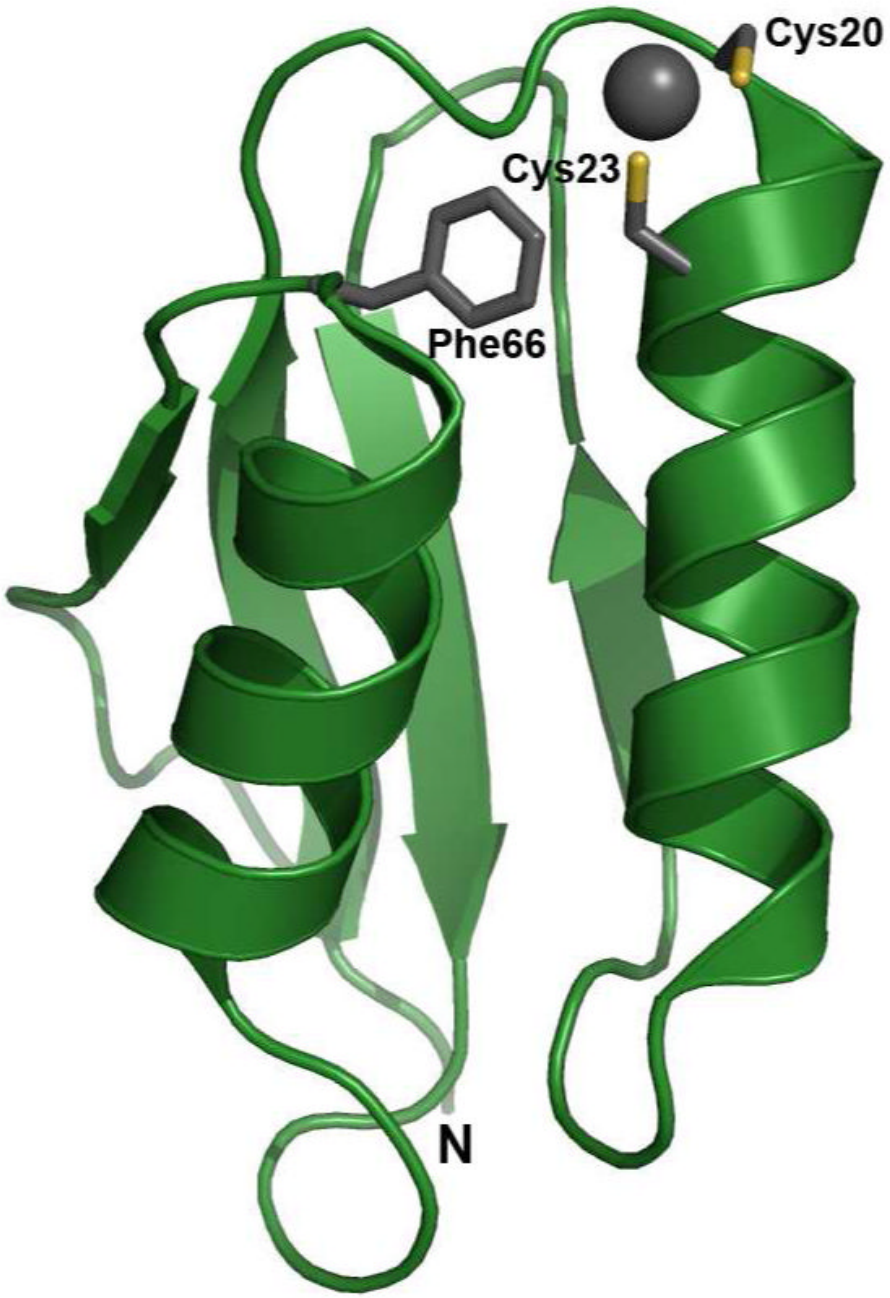

Figure 9.
Solution structure of the second MBD of the Menkes disease protein (MNK2) (PDB accession code 1S6U). The Cu(I) ion is shown as a gray sphere and coordinating cysteine residues are shown as sticks. Residue Phe66 occupies the same position as the conserved lysine residue in the Atx1-like chaperones (Figure 6).

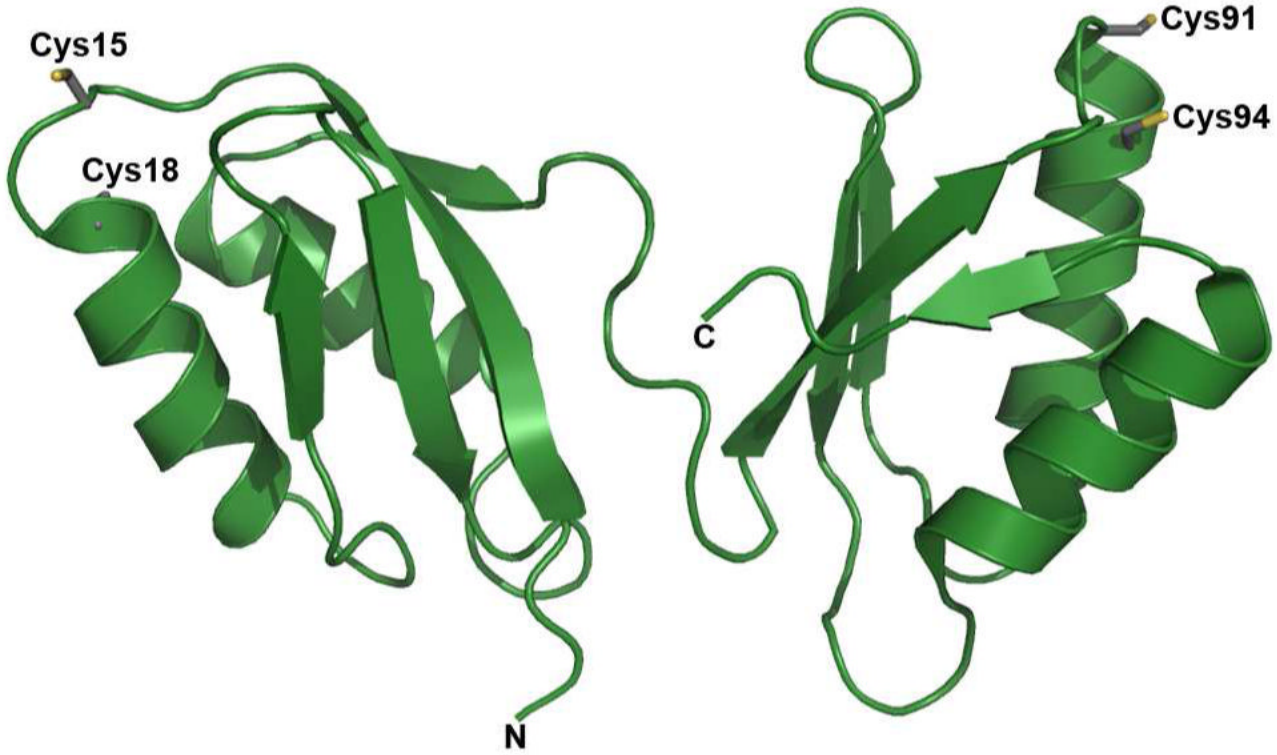

Figure 10.
Solution structure of the fifth and sixth MBDs of the Wilson disease protein (WLN56) (PDB accession code 2EW9). The two CXXC motifs are shown as sticks.

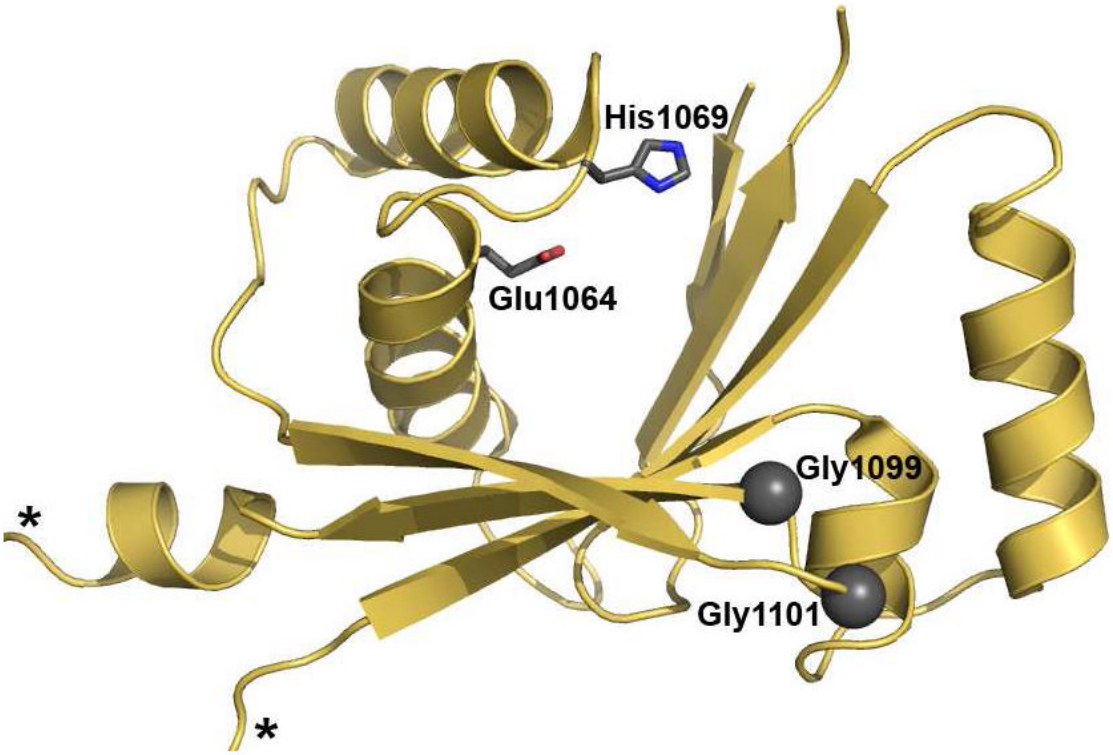

Figure 11.
Solution structure of the Wilson N domain (PDB accession code 2ARF). Invariant residues involved in ATP binding are highlighted. Residue His1069 is mutated in Wilson disease patients. The two asterisks denote the termini of an extended unstructured region.

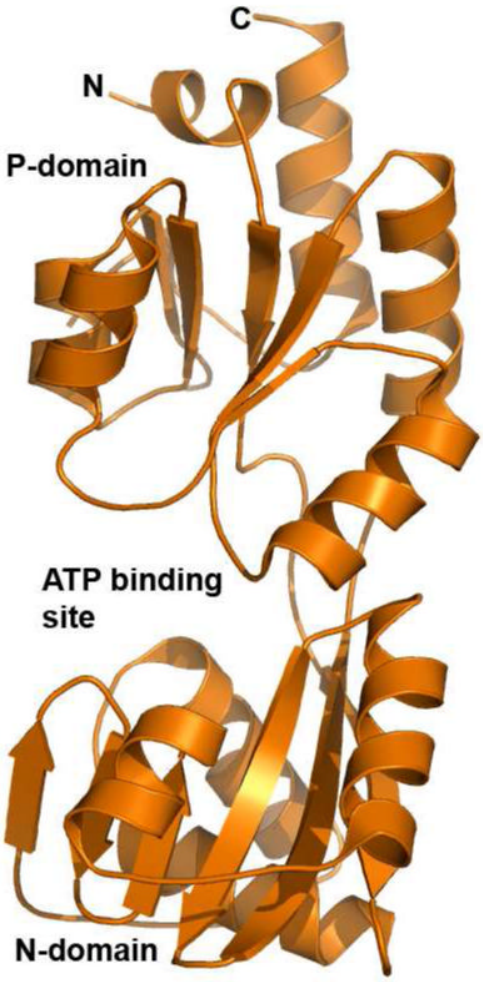

Figure 12.
Crystal structure of the ATP binding domain from *A. fulgidus* CopA (PDB accession code 2B8E). The ATP binds in a cleft between the N- and P-domains. The unstructured loop in the Wilson N-domain (Figure 11) is not present.

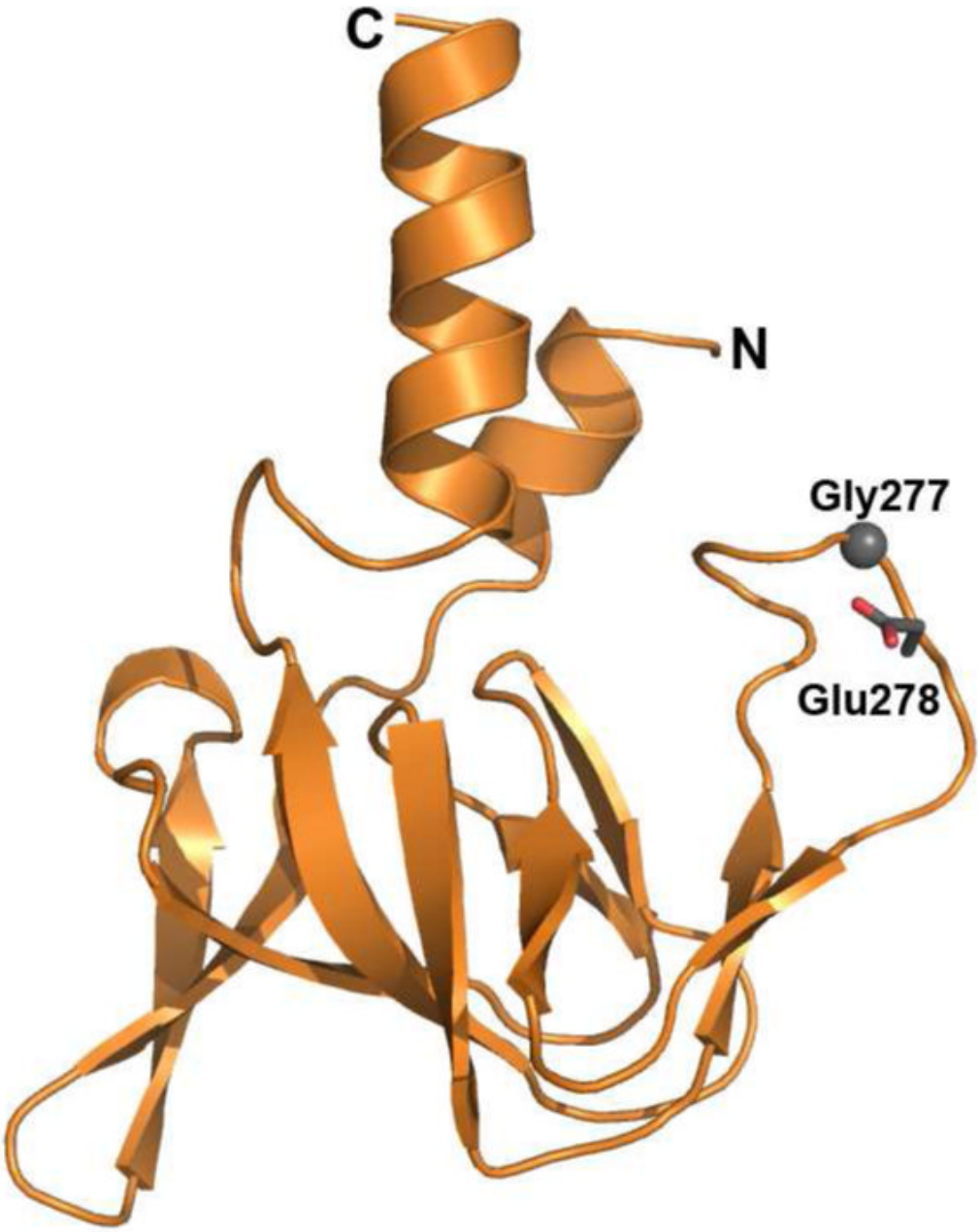

Figure 13.
Crystal structure of the A domain from *A. fulgidus* CopA (PDB accession code 2HC8). The conserved GE sequence is highlighted.

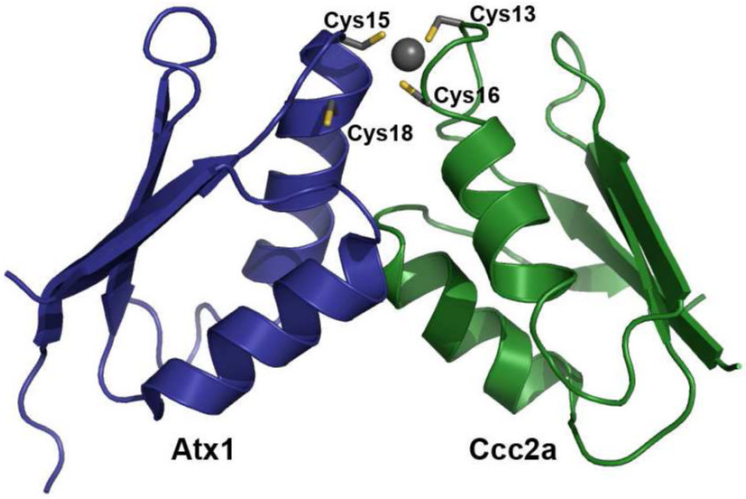

Figure 14.
Solution structure of the complex between Atx1 and Ccc2a (PDB accession code 2GGP). The Cu(I) ion is shown as a gray sphere and is coordinated by Cys15 from Atx1 and Cys13 and Cys16 from Ccc2a.

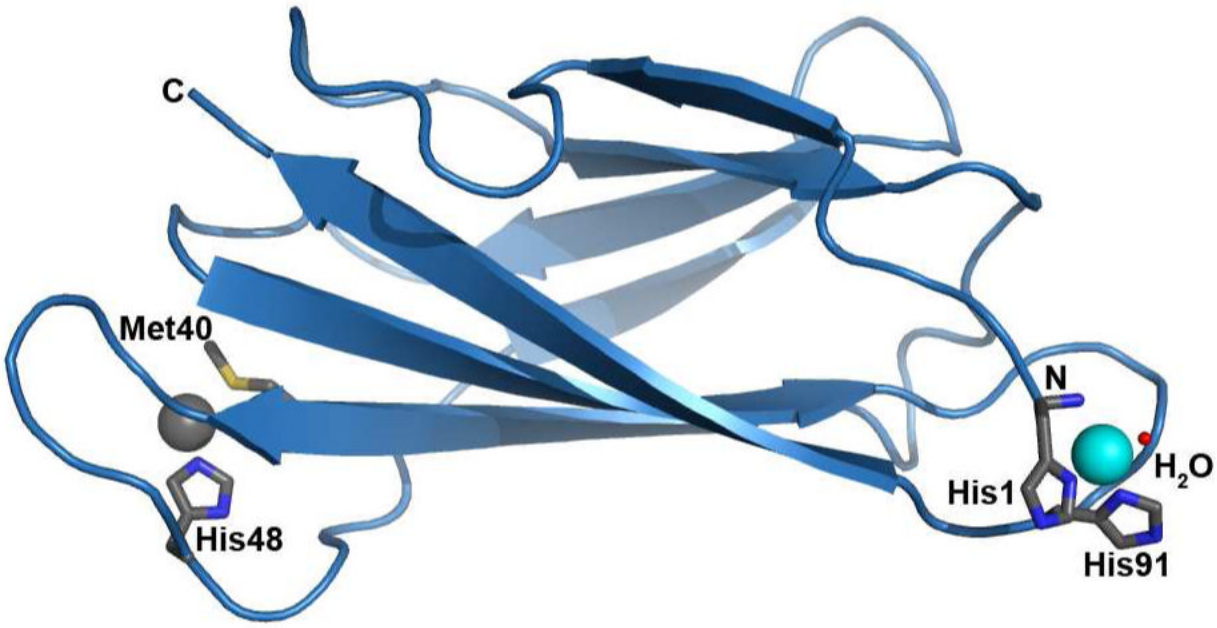

Figure 15.
Crystal structure of *P. syringae* CopC at pH 7.5 (PDB accession code 2C9Q). The Cu(I) ion (gray sphere) is coordinated by His48 and Met40. The Cu(II) ion (cyan sphere) is coordinated by the N-terminal amino group, His1, His91, and a water molecule (red sphere).

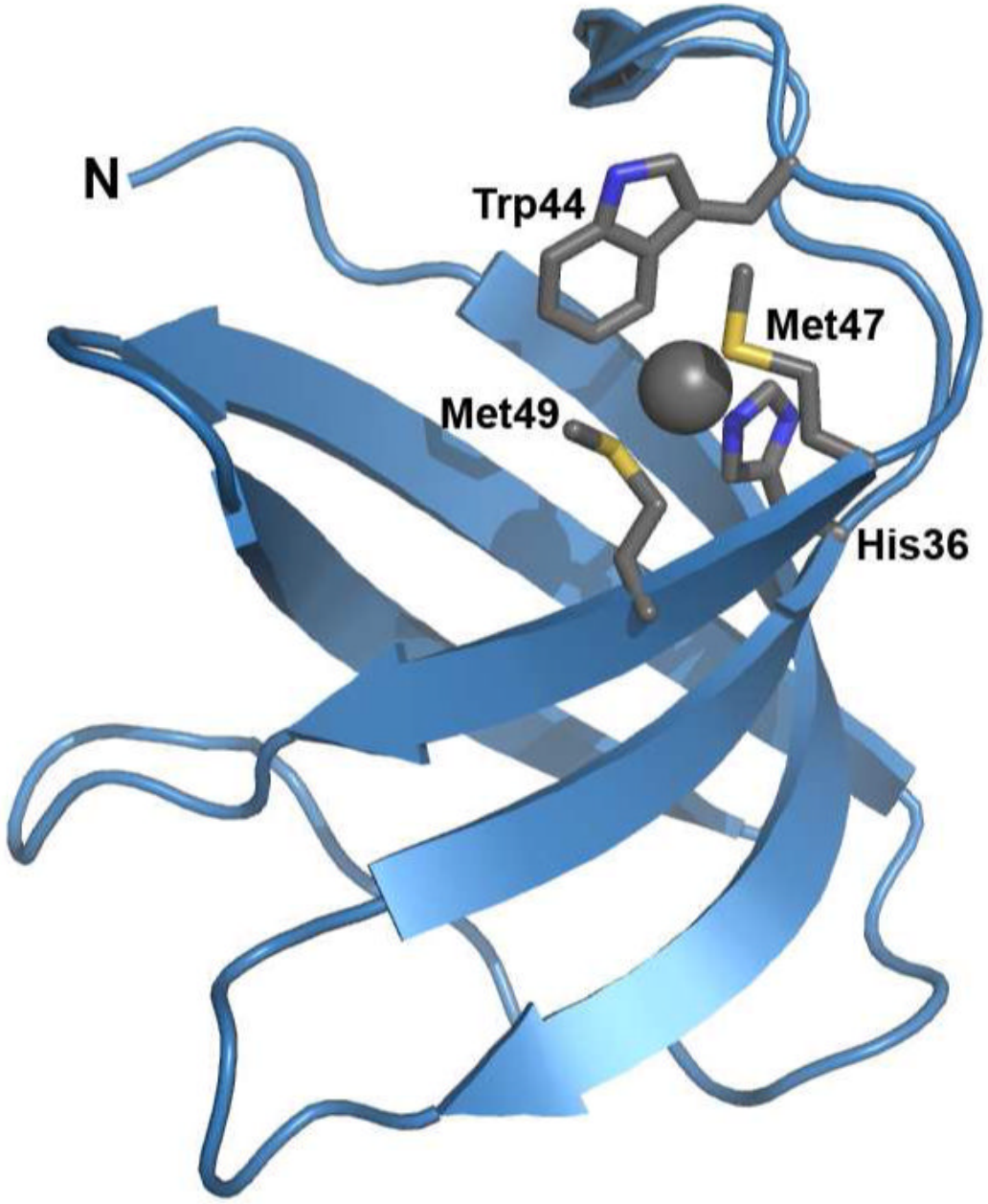

Figure 16.
Crystal structure of *E. coli* CusF (PDB accession code 2VB2). The Cu(I) ion (gray sphere) is coordinated by His36, Met47, and Met49, and interacts with Trp44 via a cation-π interaction.

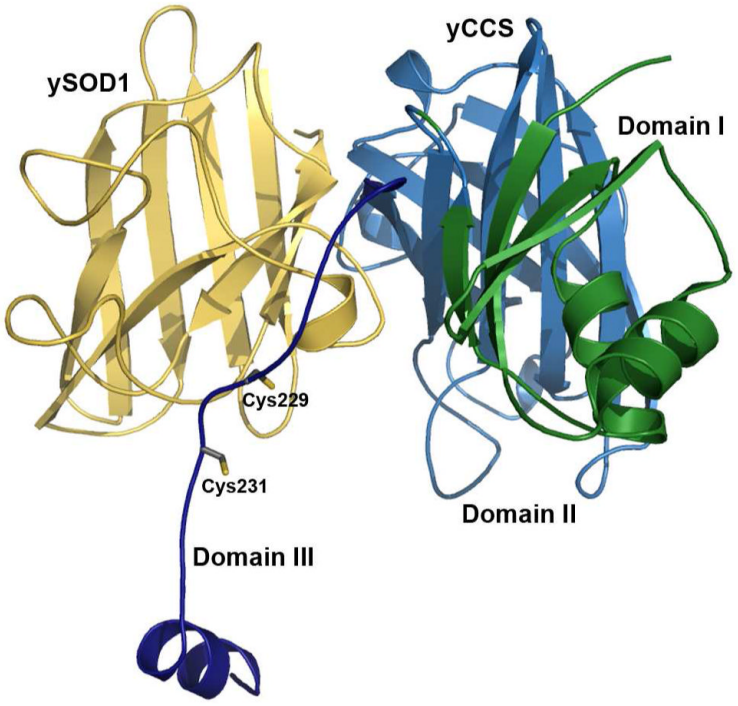

Figure 17.
Crystal structure of the complex between yCCS and ySOD1 (yellow) (PDB accession code 1JK9). Domain I of yCCS is shown in green, domain II is shown in blue, and domain III is shown in dark blue. The functionally important CXC motif in domain III is shown as sticks.

Chem Rev. Author manuscript; available in PMC 2010 October 1.

Table 1

Structures of soluble copper trafficking proteins

Organism	Protein	Type	Resolution	PDB	Ref.
Atx1-like Cu(I) chaperones					
Yeast	Hg(II)-Atx1	X-ray	1.02 Å	1CC8	81
	apo-Atx1 (ox.)	X-ray	1.2 Å	1CC7	81
	Cu(I)-Atx1	NMR		1FD8	86
	apo-Atx1 (red.)	NMR		1FES	86
Human	Hg(II)-Atox1	X-ray	1.75 Å	1FE4	93
	Cd(II)-Atox1	X-ray	1.75 Å	1FE0	93
	Cu(I)-Atox1	X-ray	1.8 Å	1FEE	93
	Cu(I)-Atox1	NMR		1TL4	94
	apo-Atox1 (red.)	NMR		1TL5	94
E. hirae	apo-CopZ	NMR		1CPZ	96
B. subtilis	Cu(I)-CopZ	NMR		1K0V	97
	apo-CopZ	NMR		1P8G	98
S. sp. PCC6803	apo-ScAtx1	NMR		1SB6	102 103
A. fulgidus	CopZ	X-ray	1.78 Å	2HU9	61
PcoC-like copper resistance proteins					
E. coli	PcoC	X-ray	1.5 Å	1LYQ	150
P. syringae	Cu(I)-CopC	NMR		1NM4	155
	Cu(II)-CopC	NMR		1OT4	157
	apo-CopC	NMR		1M42	156
	Cu(I)/(II)-CopC	X-ray	1.60 Å	2C9Q	158
	Cu(I)/(II)-CopC	X-ray	2.25 Å	2C9P	158
	apo-CopC	X-ray	2.00 Å	2C9R	158
Cus chaperones					
E. coli	Ag(I)-CusF	X-ray	1.0 Å	2QCP	162
		X-ray	2.33 Å	2VB3	163
	Cu(I)-CusF	X-ray	1.7 Å	2VB2	163
	apo-CusF	X-ray	1.5 Å	1ZEQ	161
CCS chaperones					
Yeast	apo-CCS	X-ray	1.8 Å	1QUP	168
	apo-CCS/SOD	X-ray	2.90 Å	1JK9	173
Human	apo-CCS	X-ray	2.75 Å	1DO5	172

Table 2

Structures of domains of Cu(I) transporting P_{1B}-type ATPases

Organism	Protein	Type	Resolution	PDB	Ref.
Cu(I) Transporting ATPases					
Yeast	Cu(I)-Ccc2a	NMR		1FVS	118
	apo-Ccc2a	NMR		1FVQ	118
	Atx1-Ccc2a	NMR		2GGP	145
Human	apo-MNK4	NMR		1AW0	120
	Ag(I)-MNK4	NMR		2AW0	120
	apo-MNK2	NMR		1Q8L	121
	apo-MNK2	NMR		1S6O	122
	Cu(I)-MNK2	NMR		1S6U	122
	apo-MNK1	NMR		1KVI	123
	Cu(I)-MNK1	NMR		1KVJ	123
	apo-MNK3	NMR		2G9O	124
	Cu(I)-MNK3	NMR		2GA7	124
	A69P apo-MNK6	NMR		1YJR	126
	A69P Cu(I)-MNK6	NMR		1YJT	126
	apo-MNK6	NMR		1YJU	126
	Cu(I)-MNK6	NMR		1YJV	126
	apo-WLN56	NMR		2EW9	88
	apo-WLN34	NMR		2ROP	128
	WLN N dom.	NMR		2ARF	129
B. subtilis	apo-CopAb	NMR		1JWW	133
	Cu(I)-CopAb	NMR		1KQK	133
	apo-CopAa	NMR		1OQ3	134
	Cu(I)-CopAa	NMR		1OQ6	134
	apo-CopAab	NMR		1P6T	133
	apo-CopAab	NMR		2RML	135
A. fulgidus	CopA A dom.	X-ray	1.65 Å	2HC8	140
	CopA ATPBD	X-ray	2.30 Å	2B8E	136